



McGill

Magnesium Phosphate Precipitates and Coatings for Biomedical Applications

Submitted by
Suzette Ibasco

Faculty of Dentistry
McGill University, Montreal

15 April 2009

*A thesis submitted to the Faculty of Graduate Studies and
Research in partial fulfillment of the requirements of the degree
of Master of Science in Dental Science (M. Sc.)*

Dedication

to mom, dad and kuya

*"It is my conviction that it is the intuitive, spiritual aspects
of us humans-the inner voice-that gives us the 'knowing,'
the peace, and the direction to go through the windstorms of life,
not shattered but whole, joining in love and understanding."
-Elisabeth Kübler-Ross (1926 - 2004)*

Acknowledgements

First and foremost, I would like to express my sincerest gratitude to my supervisor, Dr. Jake Barralet, who has consistently supported me throughout my master's degree with his guidance, encouragement and good source of advice. The achievement of this master's study would not have been possible without his support and feedbacks.

I am indebted to Dr. Faleh Tamimi for particularly helping me with the writing of the manuscripts. I have enjoyed working with him and I am grateful for his explanations at the technical and scientific standpoints, as well as his good sense of humour.

This work would not have been possible without the financial support of the Natural Sciences and Engineering Research Council of Canada (NSERC) Strategic Award in collaboration with Terray Corporation (Arnprior Ontario, Canada), the *Fundacion Espanola para la Ciencia y Tecnologia* (FECYT) grant, the Québec Ministère des Relations Internationales (Québec-Bavaria Exchange Program) PSR-SIIRI-029 IBI and the Canada Research Chair program.

Finally, I am most grateful for the abundant support and encouragement from my family and friends throughout my master's degree, for providing balance in my life, and making this all worthwhile.

Table of Contents

Dedication	1
Acknowledgements	3
List of Figures	6
List of Tables.....	9
Preface: Contribution of Authors	10
Abstract	11
Résumé	12
CHAPTER 1: Introduction and Research Rationale	13
CHAPTER 2: Thesis Objectives and Outline.....	15
2.1- Hypotheses.....	15
2.2- Objectives	15
2.3- Outline.....	15
CHAPTER 3: Background and Literature Review.....	17
3.1- The Skeleton	17
3.2- The Hierarchical Structure of Bone	17
3.2.1- The Cortical and Cancellous Bone.....	17
3.3- Mechanical Properties of Bone	19
3.4- Components	20
3.5- Cells	20
3.6- Need for Bone Repair	21
3.7- Grafting.....	21
3.7.1-Synthetic Bone Graft Materials.....	25
3.7.1.1-Porous Metal Foams	25
3.7.1.2-Polymers	25
3.7.1.3 Bioceramics	26
3.8- Implants.....	27
3.9- Bone-Implant Interface	29
3.9.1- Osseointegration	30
3.9.2- Types of Interface	30

3.10- Calcium Phosphate.....	36
3.11- Magnesium and Magnesium Phosphate Biomaterials	39
References.....	42
CHAPTER 4: INVESTIGATION INTO AQUEOUS MAGNESIUM PHOSPHATE PRECIPITATION FOR BIOMEDICAL APPLICATIONS	57
4.1- ARTICLE 1.....	58
4.1.1- Abstract.....	58
4.1.2- Introduction.....	59
4.1.3- Materials and Methods.....	60
4.1.4- Results.....	62
4.1.5- Discussion	72
4.1.6- Conclusion	73
4.1.7- Acknowledgement	74
4.1.8-References.....	74
CHAPTER 5: REACTIVE MAGNESIUM SPUTTERED TITANIUM FOR THE FORMATION OF BIOACTIVE COATINGS	78
5.1- ARTICLE 2.....	79
5.1.1- Abstract.....	79
5.1.2- Introduction.....	80
5.1.3- Materials and Methods.....	82
5.1.4- Results.....	86
5.1.5- Discussion	91
5.1.6- Conclusion	96
5.1.7-Acknowledgements.....	96
5.1.8- References.....	97
CHAPTER 6: Discussion and Conclusion	102
CHAPTER 7: Future Research.....	104
7.1-Preliminary <i>in vivo</i> results.....	104
7.2- Magnesium Phosphate Cements	109

List of Figures

Figure 3.1: Structure of compact and cancellous bone.....	19
Figure 3.2: Photograph image of hard tissue implants for total hip replacement and bone screws and plates for fixation devices fixation.....	27
Figure 3.3: A schematic diagram of plasma spray deposition process.....	30
Figure 3.4: A schematic diagram of plasma spray deposition process	32
Figure 3.5: SEM micrograph of an uneven coating due to change in spraying angle. <i>The arrow indicates the direction of the spray</i>	33
Figure 4.1: Magnesium phosphate precipitates as function of pH, temperature and concentration. <i>Cattiite(▲); newberyite(■) magnesium hydroxide(◆); bobierrite and holtedahlite(*); TMPP(×); no precipitate (+)</i>	64
Figure 4.2: XRD of magnesium phosphate precipitates as function of pH, temperature and concentration. <i>Cattiite(▲); newberyite(■) magnesium hydroxide(◆); bobierrite(*); holtedahlite (●); and TMPP(×)</i>	64
Figure 4.3: FTIR analysis of the precipitates obtained in concentrated solutions as a function of pH and temperature.....	66
Figure 4.4: SEM pictures of the precipitates obtained at different conditions. <i>A: Newberyite (75°C; pH 6); B: TMPP (37°C; pH 10); C: Cattiite (4°C; pH 7.4); D: Bobierrite (75°C; pH 7.4)</i>	67
Figure 4.5: Characterization of precipitates obtained at different P:Mg ratios from solutions with a $[PO_4^{2-}] = 100\text{mM}$, at pH 7.4 and 37°C. <i>A: SEM micrograph of precipitates obtained at $[P:Mg] = 1.0$. B: SEM micro graphs of precipitates obtained at $P:Mg = 4$</i>	68
Figure 4.6: A: TEM micrograph; and B: TEM electron diffraction, of newberyite nanocrystals precipitated from solutions with a P:Mg ratio of 4; at pH 7.4 and 37°C.....	68
Figure 4.7: Graph of LDH cytotoxicity tests which revealed the magnesium phosphate powders to be non-toxic to pre-osteoblast cell line for 12h.....	70
Figure 4.8: SEM micrographs of differentiated osteoblasts on newberyite ($25\text{mM}[Mg^{+2}]$; $100\text{mM}[PO_4^{-3}]$ solution; pH 7.4; 21°C).....	70

Figure 4.9: In vitro study of osteoblast cell culture on newberyite matrices prepared from a 67mM $[Mg^{+2}]$; 100mM $[PO_4^{-3}]$ solution; pH6; 55°C. A: Photograph showing cell mediated clustering of newberyite crystals. B: Optical micrograph graph showing osteoblast (Black arrows) adhering and attaching newberyite crystals together. C: Microscopic picture of osteoblast (stained with, methylene blue) colonizing the surface of newberyite. D: SEM micrographs showing the adhesion and spreading of osteoblasts over newberyite crystals.....71

Figure 5.1: A-C) SEM images of magnesium coated metals immersed in 3 component combinations, D) 4 component combination E) SBF and F) PBS.....86

Figure 5.2: SEM micrographs of Mg sputtered titanium sheets after immersion in ADP solutions for periods of 30 seconds (A); 2 minutes (B); 15 minutes (C); and 2 hours (D).....87

Figure 5.3: SEM, EDX and XRD analysis of (A,C,E) struvite coated sample before and (B,D,F)after additional coating with calcium phosphate solution. (*) indicate struvite peaks diffraction peaks (+) indicate hydroxyapatite peaks.....88

Figure 5.4: SEM micrographs and linear EDX analysis of the sample cross section: A)Mg sputtered coated titanium; B) struvite coated titanium; and C) HA coated titanium.

Figure 5.5: A) AFM images of the struvite crystals and B) the calcium phosphate platelet crystals secondary coating.....89

Figure 5.5: A) AFM images of the struvite crystals and B) the calcium phosphate platelet crystals secondary coating.....90

Figure 5.6: A) and B) SEM micrographs of pre-osteoblastic cells adhered onto struvite-calcium phosphate coating after 8 days. C) 2h cell attachment test. D) Live/Dead Viability/cytotoxicity Assay.....91

Figure 5.7: Proposed mechanism of: A) struvite coating formation on magnesium sputtered titanium after placement in ADP solution; B) and the subsequent transformation into hydroxyapatite after incubation in CaP solution.....93

Figure 7.1: Comparison of percent weight loss after four weeks implantation of alloyed and coated magnesium. Note: Pure magnesium is not included as it corroded too rapidly.....106

Figure 7.2: X-ray images of implants *in vivo*. *However, due to the low radiopacity of magnesium, the samples could not be observed under X-Ray images.*.....107

Figure 7.3: SEM micrographs and EDX analysis of A) low grade magnesium alloy and B) coated magnesium before and after four weeks implantation.....108

List of Tables

Table 3.1: The structural levels of bone adapted by An and Draughn, 2000.....	18
Table 3.2: Biomechanical properties of bone adapted from Van Audekercke and Martens, 1984.....	20
Table 3.3: Bone Graft Materials Classified by Composition as adapted from Bauer and Muschler 2000.....	23
Table 3.4: Types of biomaterials for bone repair adapted from Murugan and Ramakrishna, 2004.....	24
Table 3.5: Different Techniques to deposit CaP/HA <i>coatings (modified after Yang et al. 1999)</i>	34
Table 3.6: Properties of the biologically most relevant calcium orthophosphates with decrease in resorbability.....	38
Table 3.7: Comparison of different form of grafts; cement, granules and blocks.....	38
Table 3.8: Magnesium phosphate precipitation reactions in aqueous solutions with their respective solubility.....	41
Table 4.1: Density and ICP Measurements for samples prepared in concentrated solutions.....	69
Table 5.1: Composition and concentrations (mM) of the reacting solutions.....	83

Preface: Contribution of Authors

This master's thesis is a compilation of two manuscripts, (one submitted and one in preparation) by the candidate as first author and selected highlights of preliminary studies. Preparation and execution of the experiments, in particular the precipitation of the magnesium phosphate powders and coatings of the metals, as well as the characterization and analyses have been performed by the main author. Contribution of the listed coauthors includes that of Mr. Meszaros who performed the preliminary experiments and Dr. Tamimi who was mainly involved with technical advice and assistance as well as manuscript preparation. The help of Drs. Gbureck and Knowles included the initial collection of the x-ray diffraction patterns of the magnesium phosphate powders, whilst the cell tests were performed under the guidance of Dr. Le Nihouannen. The help of Dr. Vengallatore for the sputtering of the titanium substrates as well as the consulting expertise of Dr. Harvey have been most helpful. Finally, the achievement of this thesis would not have been possible without the supervision and constant guidance of Dr. Barralet.

Abstract

Metals are extensively used materials in orthopaedics and oral implants and several research studies have reported that coating the surface improves the osteoconduction and bone bonding ability of the metal. Low temperature aqueous precipitation techniques are advantageous over other coating processes as they allow the incorporation of thermally unstable compounds. Although some magnesium phosphates have been shown to be well tolerated in bone tissue [Zimmermann 2006], they are relatively unstudied as bioceramics. The first part of this research project was to determine the precipitation conditions at which different magnesium phosphate phases form. Ultimately, the primarily goal of this study was to investigate a new low temperature route to produce magnesium phosphate coatings by reacting substrates sputter coated with magnesium metal in an aqueous phosphate solution.

X-ray diffraction (XRD) and scanning electron microscopy (SEM) coupled with energy dispersion spectroscopy (EDS) were used to characterize and identify the magnesium phosphate precipitates. SEM revealed that coatings formed by the reaction of magnesium metal with ammonium dihydrogen phosphate formed a continuous coating of struvite crystals. Importantly, this coating was durable enough to withstand the peel test (ASTM D 3359). Furthermore, this coating was also useful as a reactive surface to form hydroxyapatite coating. Biocompatibility assays, showed that magnesium phosphates precipitates and coatings were non-toxic and sustained cell viability. This study shows the possibility of forming a number of potentially biocompatible surface coatings on a metal model through a low temperature *in situ* process. This process shows good promise in producing enhanced coatings with many advantages over currently used techniques.

Résumé

Les métaux sont largement utilisés comme matériaux dans la conception d'implants orthopédiques et dentaires et plusieurs études ont montré qu'un revêtement de leurs surfaces améliore leur propriété d'ostéoconduction et leur capacité de liaison au tissu osseux. Les techniques de précipitation aqueuse à basse température sont plus élaborées comparées aux autres techniques de revêtement car elles permettent l'incorporation de composés thermiquement instables. Bien que certains phosphates de magnésium soient bien tolérés au sein du tissu osseux [Zimmermann 2006], ils sont relativement peu étudiés comme biocéramiques. La première partie de ce projet de recherche était de déterminer les conditions de précipitations auxquelles les différentes phases des phosphates de magnésium se forment. L'objectif majeur de cette étude était d'explorer une nouvelle méthode, à basse température, pour produire des revêtements de phosphate de magnésium par la réaction de substrats revêtus par pulvérisation avec des métaux magnésiens, dans une solution aqueuse de phosphate.

La diffraction des rayons X et la microscopie électronique à balayage, couplée à la spectrométrie par dispersion d'énergie, furent utilisées pour caractériser et identifier les précipités de phosphates de magnésium. La microscopie électronique à balayage a révélé que les revêtements produits par la réaction d'un métal magnésium avec un phosphate diacide d'ammonium forment un revêtement continu de cristaux de struvite. Ce revêtement présentait également la caractéristique majeure de résister au test d'arrachage. Les tests de biocompatibilité ont montré que les précipités de phosphates de magnésium ainsi que les revêtements de surface étaient non toxiques et amélioraient la viabilité cellulaire. Cette étude démontre la possibilité de former un éventail de revêtements potentiellement biocompatibles à la surface d'un métal standard, à travers un procédé *in situ* à basse température. Ce procédé présente des perspectives intéressantes pour la production de revêtements plus performants, en montrant également de nombreux avantages sur les techniques actuellement employées.

CHAPTER 1: Introduction and Research Rationale

Bone diseases and fractures count for half of all chronic diseases in the population over 50 years of age in developed countries. Moreover, the prevalence of these problems is likely to increase in the nearby future due to the aging of the population [Bone and Joint Decade's Musculoskeletal Portal, 2007]. These diseases cause high morbidity, and often require surgical interventions.

Currently stainless steel, titanium and cobalt chrome alloy are used as plates and screws to immobilise fractures in load bearing sites. Degradable polymers such as polylactic acid are used only in non-load bearing situations mainly confined to the craniofacial region. Two very attractive features of a degradable metallic fixation material are firstly that load will be transferred from the fixation device to the bone during healing, thus preventing stress shielding and secondly an additional operation to remove the fixation plate after healing could become unnecessary. The potential use of magnesium alloys as a biodegradable metal for internal fixation has been sporadically investigated for 100 years, yet has to date failed to find commercial application. Magnesium's negligible toxicity encouraged its pioneering use as plate for fracture fixation in 1907. The pure magnesium plate was fixed with gold-plated steel nails; however, rapid corrosion of the metal *in vivo* produced a large amount of gas beneath the skin that caused its eventual failure [Lambotte 1932]. In order to control magnesium corrosion rate *in vivo*, alloying with other metals, as well as alkali coatings have been assayed. Magnesium stents alloyed with rare earth elements (7 wt.%) have shown great potential in cardiovascular surgery. Future work in enhancing the corrosion resistance of this material is under development to be used as orthopaedic implants. However, early dissolution rates have been observed on all cases and are too high to eliminate rapid gas formation. A review of the literature indicates that hydrogen gas production has always been observed following *in vivo* implantation of magnesium but it is highly significant that gas formation is not continuous and is most commonly noted in the first few days of implantation [Witte *et al.* 2005].

Magnesium phosphates such as Newberyite ($\text{MgHPO}_4 \cdot 3\text{H}_2\text{O}$) are formed biologically and are known to be degradable and non toxic when implanted *in vivo* [Driessens 2005]. Indeed magnesium apatites have been shown to support osteoblast differentiation and function [Zreiqat *et al.* 2005].

Based on the observation that phosphate coatings have been reported following *in vivo* implantation of magnesium metals [Witte *et al.* 2005] and that close bone apposition occurred on these corrosion products, we will explore the unique ability of pre-corrosion of magnesium coatings. This approach should reduce the *in vivo* degradation rate of magnesium metal and also eliminate initial gas production that is present initially following implantation. This study provides new information on the formation conditions of magnesium phosphates as well their use as insoluble coatings on metallic fixation devices (i.e. titanium implants) both *in vitro* and *in vivo*.

CHAPTER 2: Thesis Objectives and Outline

2.1- Hypotheses

1) In addition to Newberyite, other magnesium phosphates may have potential as either degradable or non degradable biomaterials that may have application in hard tissue repair

2) The reaction of magnesium metal with phosphate containing solutions may offer a route to produce novel low temperature coatings for metallic implants.

2.2- Objectives

In order to explore hypothesis (1) magnesium phosphates precipitates were formed over a range of temperature, pH and concentration and their potential as bioceramics was investigated. To determine whether hypothesis (2) could be valid, magnesium sputter coated metal substrates were produced with the objective of reacting these coatings in aqueous conditions to form stable phosphate coatings.

2.3- Outline

This thesis is prepared in a manuscript format and is divided into seven chapters., the first two being Introduction and Objectives. Chapter 3 consists of a literature review in which bone anatomy and associated mechanical properties are reviewed. Current and potential treatment options for bone disease and fractured bone are discussed, and more specifically the role of synthetic grafts as a suitable alternative to the more commonly

used autograft in surgical procedure is outlined. Furthermore, an overview and comparison of the most commonly used techniques and materials for coating metallic implants to improve the biocompatibility, osteoconduction and the physical bond between the implant and host tissue. Finally, the potential use of coating with magnesium phosphate bioceramics is reported as an alternative to the commercially used plasma spraying with hydroxyapatite method.

Chapters 4 and 5 present two papers one submitted for the peer reviewed journal Acta Biomaterialia and the second in preparation. The first article (Chapter 4) investigates the occurrence of the types of magnesium phosphate precipitated at different conditions. The second article (Chapter 5) evaluates a new low temperature route to produce ammonium magnesium phosphate coatings by reacting magnesium sputter coated titanium metal in different phosphate solutions. The different magnesium phosphate precipitates and coatings were characterized in terms of morphology and composition using microscopy and chemical analyses. Both articles further discuss the cytotoxicity effect and viability of these magnesium phosphate biomaterials with pre-osteoblast cells, both *in vitro* and *in vivo*.

Chapter 6 discusses the findings of these two articles and draws general conclusions from the results collected during this Master's degree. Chapter 7 reports preliminary *in vivo* results of the magnesium implants and proposes possible directions for the continuation of the research project.

CHAPTER 3: Background and Literature Review

3.1- The Skeleton

The skeleton has six main functions; support, movement, protection, blood cell production, storage and endocrine regulation. Bone provides the framework which supports the body and maintains its shape. In order for motion to occur, bone is the leverage powered by skeletal muscles that are attached to the skeleton by tendons. The skeleton also protects many vital organs. For instance, the skull protects the brain, the spine protects the spinal cord and the rib cage protects the lungs, heart and major blood vessels. The bone is also the site of haematopoiesis, which occurs in the red bone marrow. The skeleton matrix can also store calcium and iron for metabolism [Gray's Anatomy, 2008]. Bone cells release osteocalcin hormones which controls the regulation of glucose and fat deposition. Osteocalcin also increases the secretion of insulin and insulin producing cells [Lee, 2007].

3.2- The Hierarchical Structure of Bone

The following section will cover a brief overview of the main structural levels of bone in the body as summarized in Table 3.1. Due to the scope of this thesis, this chapter will mainly address the cortical and cancellous bone structures as shown in Figure 3.1.

3.2.1- The Cortical and Cancellous Bone

Cortical Bone

Bones are generally comprised of one or both of two distinct types, namely, cortical and cancellous bone. The bone consists of a basic double structure, the cortical and the cancellous part, which changes in proportion depending on the age, disease, function and anatomical site. The cortical bone tissue is smooth, continuous and dense, and is located on the outer layer of the bone. It consists of tightly packed cylindrical elements called osteons, which are composed of a central canal (Haversian) that are

Table 3.1: The structural levels of bone adapted by An and Draughn, 2000.

Level	Elements	Main Factors determining Bone Strength
Macrostructure (whole bone)	Femur, humerus, vertebrae, frontal, etc.	Macrostructure such as tubular shape, cross-sectional area, and porosity of long bone, cortical bone-covered vertebrae, or the irregular pelvic bone
Milliscale (tissue)	Compact or Cancellous bone blocks, cylinders, cubes or beams	Density, porosity, osteon orientation, collagen fibre or trabeculae
Microstructure (osteonal/trabecular)	Osteons, trabeculae	Loading direction
Submicrostructure (lamellar)	Lamella, large collagen fibres	The longitudinal direction of the collagen fibres
Ultrastructure (nanostructure)	Collagen fibril and molecule, mineral components	Combination of rigid HA and flexible collagen

surrounded by concentric rings of lamellae. Between these rings, there are spaces called the lacunae where bone cells (osteocytes) reside. To provide passageways through the hard cortical matrix, the Harvesian canals are linked with small channels called canaliculi in the lacunae site. The Harvesian canals which contain the blood vessels are then interconnected via *Volkmann's* canals with vessels on the surface of the bone. [Gray's Anatomy, 2008]

Cancellous Bone

The inner cancellous part of the bone is light and porous. It is arranged in a network of intersecting plates (trabeculae) and spicules. The trabeculae are organized following the lines of stress and can realign with the direction change of the stress to provide maximum strength. These cavities are filled with blood vessels and bone marrow and are interconnected with the canaliculi (Figure 3.1).

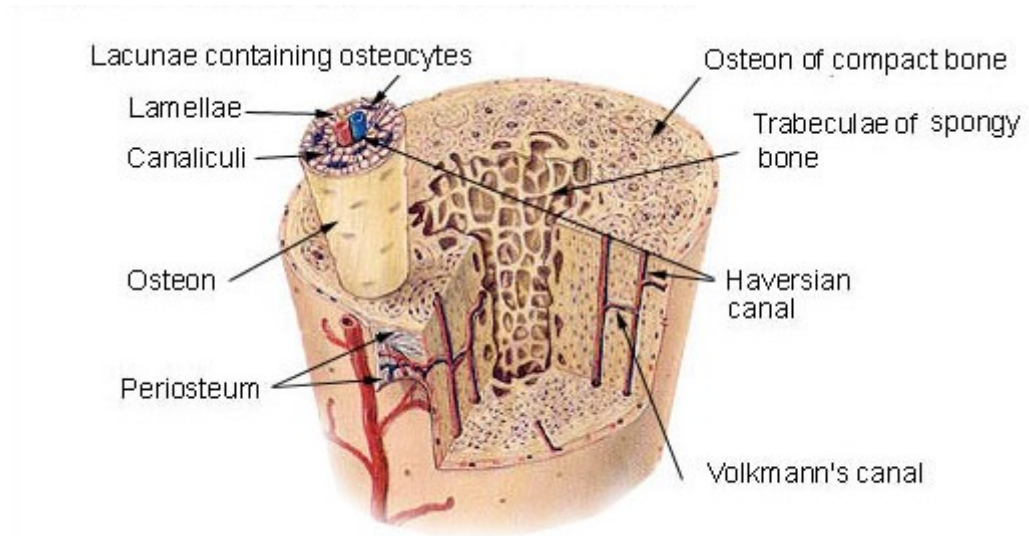


Figure 3.1: Structure of compact and cancellous bone [Young *et al.* 2000].

3.3- Mechanical Properties of Bone

The unique combination of hard inorganic and tough organic materials produces excellent mechanical properties. For instance, as shown in Table 3.2, compact bone has been reported to reach tensile strengths in the range of 50-150 MPa and a compressive strength in the range of 170-193 MPa [Bonfield, 1984]. The tensile mechanical properties of both aluminum and mild steel are within the same range, however, bone is significantly lighter. Being a natural material, measured strengths of bone vary depending on scale sample, orientation, etc. (see Table 3.2). The highest strength of bone is along the longitudinal axis, which is nearly parallel to both the collagen fibres and the long axis of the mineral crystals. Bone is stiff but also demonstrates an extensive amount of elasticity, which is crucial during impact. The modulus of elasticity of bone specimens has been shown to be in the range of 14-20 MPa [Bonfield, 1984], which is much less than steel. Bone is also a tough material having values within the range 2-12 MPa m^{1/2} in comparison to 0.7-1.0 MPa m^{1/2} for silicate glasses [Morena *et al.*, 1986].

Table 3.2. Biomechanical properties of bone adapted from Van Audekercke and Martens, 1984.

Properties	Measurements		
	Cortical Bone	Reference	Cancellous Bone
Young's modulus (GPa)	14–20	[Bonfield, 1984]	0.05–0.5
Tensile strength (MPa)	50–150	“	10–20
Compressive strength (MPa)	170–193	“	7–10
Fracture toughness (K_{Ic} : MPa m ^{1/2})	2–12	“	0.1
Density (g/cm ³)	18–22	“	0.1–1.0

3.4- Components

Bone is a highly complex natural composite material composed of inorganic (70 wt %), and organic (20 wt %) material, ground substance (8 wt. %) and water (2 wt %). The organic matrix consists of 95 wt % of type-I collagen fibrils and of proteoglycans and numerous non-collagenous proteins (5wt %). The ground substance consists of bone cells which is discussed more in debt in the following section. The inorganic phase in bone is hydroxyapatite (HA: $(Ca_{10}(PO_4)_6(OH)_2)$ substituted with trace amounts of other ions associated with physiological fluids. The various ions found in bone mineral are; 0.5 wt % Mg, 0.8 wt % Na, 0.2 wt %K, 8.0 wt %CO₃, 0.2 wt % Cl and 0.08 wt % F [Aoki, 1991].

3.5- Cells

There are three main types of bone cells; osteoblasts, osteocytes and osteoclasts. Osteoblasts are responsible for bone matrix synthesis and are mainly found at bone surfaces forming a continuous layer. They synthesize and secrete a collagen type-I rich substance into a region of unmineralized matrix and form osteoid. Osteoblasts then cause calcium and phosphate to precipitate and combine with osteoid for bone mineralization. Osteoclasts, on the other hand, play a key role in bone resorption once bone matures. They adhere on the bone surface undergoing resorption and secrete bone reabsorbing

enzymes, which digest the bone matrix. Osteocytes are osteoblasts that have been encapsulated in mineralised tissue (lacunae). They play a key role in maintaining bone and are usually found within the bone matrix. They control the extracellular level of calcium and phosphate. Hence, for proper skeletal growth and mechanical function, bone undergoes a dynamic remodelling cycle via resorption by osteoclasts and reformation by osteoblast cells [Buckwalter *et al.*, 1996].

3.6- Need for Bone Repair

“The World Health Authority has decreed that 2000–2010 will be the Bone and Joint Decade, and this is now being supported by the United Nations” [Lidgren, 2003]. Bone and joint diseases affect millions of people worldwide where they account for half of all chronic diseases in people over 50 in developing countries. The most common causes of bone defects include trauma (i.e. motor vehicle collisions, pedestrian/vehicle accidents, ballistic injuries), birth defects (i.e. nasoalveolar cleft, craniofacial deformities), tumours and diseases (i.e. periodontitis, osteoarthritis, osteoporosis). Approximately 30 000 hip fractures have been reported every year in Canada alone, of which some 6000 may die [Seiberling, 2007]. It is estimated that 25% of health costs in developing countries will be spent in trauma-related care by the end of the decade. Periodontal disease, which is the occurrence of infected gums with bone loss, is the most common cause of alveolar bone resorption. Furthermore, *Osteoporosis Canada*© has quoted that osteoporotic fractures have doubled in the last decade.

3.7- Grafting

Every year around the world, it is estimated that over 2 million bone graft operations are performed, where 90% use natural bone from autografts or allografts and the remaining 10% use synthetic materials [White *et al.* 2007]. The use of autografts is considered to be the “gold standard” for bone repair when compared with allografts and synthetic grafts as they have the capacity to induce angiogenesis and support extensive bone remodelling [Ito *et al.*, 2005]. They also do not elicit any immunogenic reaction after surgery and have shown good osteoconductivity [Coombes and Meikle, 1994. Yaszemski *et al.*, 1996. Cornell and Lane, 1998.].

In the event of bone disease or injury, bone grafts have served as both mechanical and biological roles to restore skeletal integrity, fill voids, and enhance bone repair. There are four types of bone grafts: autograft, allograft, xenograft and synthetic materials (Table 3.3).

Autograft is defined as bone tissue that is harvested and implanted on a different site in the same individual. They can either be aspirated bone marrow, cancellous, cortical or vascularized bone. Autografts are usually harvested from the iliac crest of the patient, where their uses have been reported for numerous applications including anterior cervical spine fusion [Parthiban *et al.* 2002]. Bone from the tibia and fibula have also been used as autografts but to a lesser extent.

Allograft refers to a harvested tissue transplanted between genetically nonidentical individuals of the same species. In order to reduce the host immune reaction and implant rejection, they are processed by freeze drying or demineralization and sterilized by irradiation or with ethylene oxide gas to remove the cells. Unlike viable autografts, they do not exhibit any osteogenic properties. They can come in different forms such as powder, gel, paste or blocks from cortical and cancellous bone or osteochondral site.

Xenografts are harvested tissue from a donor of a different specie to the recipient. The higher risk of immune response associated with this graft restricts most of their use. Xenografts that have been deproteinated and defatted exhibit a lower immune reaction, but also destroy osteoinductive proteins [Elves *et al.* 1974]. One of the rare types of xenograft is processed bovine collagen from bone or skin which can be prepared as gel powder, sponge or paper sheet.

Table 3.3: Bone Graft Materials Classified by Composition as adapted from Bauer and Muschler 2000.

Autograft	Allograft	Synthetic skeletal materials
1. Aspirated bone marrow or processed osteogenic cells 2. Cancellous bone 3. Monovascularized cortical bone 4. Vascularized bone	1. Graft Anatomy i) Cortical ii) Cancellous iii) Osteochondral 2. Graft processing i) Fresh ii) Frozen iii) Freeze-dried iv) Demineralized 3. Graft sterilization i) Sterilely processed ii) Irradiated iii) Ethylene oxide 4. Handling properties (packaged product) i) Powder ii) Particulate iii) Gel iv) Paste or putty v) Chips vi) Strips or blocks vii) Massive	1. Osteoconductive blocks or granules 2. Osteoconductive cements 3. Osteoinductive proteins 4. Composites

The use of human bone is ideal for bone replacements. However, autografts are not always readily available and require additional healing due to a second surgery. After surgery, various problems have also been reported such as pelvic instability, fatigue fracture [Prolo *et al.* 1985], iliac hernia [Cowley *et al.* 1983 and Challis *et al.* 1975], fistula and ureteral injury [Escalas *et al.* 1977]. Allografts can involve the risk of viral infection, implant rejection and resorption caused by immunological responses. These types of grafts would also need to undergo a sterilization process prior to surgery. In fact, tissue rejection has been associated with the use of ethyl oxide gas and gamma radiation sterilization techniques as it can alter the material properties of the grafts [Miller *et al.*

2002 and Harner *et al.* 1996]. Therefore, the need for bone grafting to replace missing hard tissue produced an increasing demand for synthetic bone grafts. The following section will describe three types of synthetic materials used as grafting materials which include, metals, polymers and bioceramics as summarized in Table 3.4.

Table 3.4: Types of biomaterials for bone repair adapted from Murugan and Ramakrishna, 2004.

Biomaterials	Advantages	Disadvantages	Applications	Examples
Metals and alloys	strong, tough, ductile	Too stiff, may corrode	Bone plates, load-bearing bone implants, dental arch wire, and dental brackets	Titanium, stainless steel, Co–Cr alloys, and Ti alloys
Ceramic	Bioinert	Brittle, poor tensile, low toughness, lack of resilience	Hip joints and load bearing bone implants	Alumina, zirconia
	Bioactive		Bone filler, coatings on bio-implants, orbital implant, alveolar ridge augmentation, maxillofacial reconstruction, and bone tissue engineering	HA, bioglass, TCP
	Bioresorbable			
Polymer	High wear resistance			
	Flexible, resilient, surface modifiable, selection of chemical functional groups	Susceptible to creep, may generate wear particles	Bone tissue scaffolds, acetabular cups, bone screws, pins, bone plates, bone and dental filler, and bone drug delivery	Collagen, gelatin, chitosan, alginate, PLA, PGA, PLGA, PMMA, PE

3.7.1-Synthetic Bone Graft Materials

3.7.1.1-Porous Metal Foams

The use of metallic foams, such as titanium and tantalum, are advantageous as they allow for bone ingrowth, mechanical interlocking with the host tissue and can be tailored to the desired density to control the mechanical properties (strength, moduli, etc.) of the material [Wheeler, 1983]. The low stiffness of titanium foams has also been desirable to reduce the stress-shielding effect [Simske 1997]. One of the earlier uses of porous metals for osseointegration was done by Weber and White in 1972. Numerous works have been subsequently reported on porous metallic materials, which demonstrated in animal studies to enable tissue ingrowth [Hahn 1970, Hirschhorn 1971, Karagiennes 1973]. More recently, titanium foams as dental screw implants are being assessed by researchers at the National Research Council (NRC) in Canada [NRC, 2005]. Furthermore, *in vitro* test with human osteoblasts have demonstrated differentiation into mature bone cells and have potential applications for spine fusion for instance [St-Pierre 2005]. However, one of the main concerns of these metal foams is that they are unresorbable and therefore remains permanently in the body which can lead to toxicity by metal ions due to corrosion [Rubin and Yaremchuk 1997]. In fact, the increase in surface areas of porous implants also accelerates the corrosion rates compared to non porous-coated implants [Ducheyne, 1983]. They also have poor wear properties and have higher elastic modulus relative to bone, which leads to the distribution of heterogeneous stress.

3.7.1.2-Polymers

Polymers are predominantly used as bone grafting material due to their biocompatibility, design flexibility, functional groups availability, surface modifiability, light weight and ductile nature [Murugan and Ramakrishna, 2004]. They can either be non-biodegradable (e.g. poly(ethylene) (PE), poly(ethylene terephthalate) (PET) and polymethylmethacrylate (PMMA)) or biodegradable (e.g. collagen, gelatin, poly(lactic acid) (PLA) and poly(lactic-co-glycolic acid) (PLGA)). The non-biodegradable polymers, such as the previously mentioned PMMA (acrylic bone cements) plays a key role in

anchoring and fixing the prosthesis to the bone. More recently, it has been used in vertebroplasty to strengthen weakened vertebral body [Phillips 2003]. It is also used to fill bone defects such as in the case for bone reconstruction at distal femur site [Asavamongkolkul *et al.* 2003] by virtue of its low toxicity and moderate strength.

The other group of polymers are the biodegradable ones. The mechanism of biodegradation is usually by hydrolysis of the polymer chain backbone to form acidic monomers, such as lactic or glycolic acids in the case of PLA and PGA respectively. In rare cases, biodegradation can also be done by cellular and enzymatic pathways [Vert and Li 1992, Li and McCarthy 1999]. Biodegradable polymers are used to repair bone. The most frequent application is in ligament tendon degradable fixation screws. In fact, one of the main advantages of polymers is that they can be easily tailored to the desired hydrophobicity and crystallinity by modifying their surface and functional groups. For instance, the use of PLG has been suitable for drug delivery [Rokkanen, 1998], bioresorbable fixation devices and bone regeneration [Middleton and Tipton, 2000]. Other degradable polymers such as PLA, PGA and PDS have found applications as bone fixation devices [Ciccone *et al.* 2001].

3.7.1.3 Bioceramics

For the application of bone grafts, perhaps the most important biological property of some bioceramics is osteoconduction which is defined as the ability of some materials to serve as a scaffold to permit the infiltration of bone cells and nutrients [Cornell and Lane 1998].

The most commonly used ceramics are alumina, zirconia and many calcium phosphates. They can either be bioinert (alumina, zirconia), bioactive (HA, bioglass) or bioresorbable (tri-calcium phosphate (TCP)) [Murugan and Ramakrishna 2005]. The excellent bioactivity of HA and bioglass have made them more suitable for bone graft substitute and implant coatings as they provide osteointegrative stimuli. The other type of bioceramics is the bioresorbable ones, where one of the most common is TCP. However, the rate of bioresorption of TCP is still not well controlled [Bohner, 2000].

Hydroxyapatite similar in structure, although not in composition to bone mineral, is by far the most studied ceramic for bone repair. It is used in several forms, ranging from granules, blocks and cements and is derived from various sources such as bovine bone, chemical synthesis and mineral conversion. Bioceramic bone grafts will be discussed in greater detail in section 3.10.

3.8- Implants

Bone defects caused by trauma, developmental deformities, tumours and diseases have consistently challenged the skills of orthopaedic and maxillofacial surgeons. There are many types of orthopaedic implants, however material considerations are similar for most of them and a typical metallic hip prosthesis will need to exemplify the use of different implant materials. There are 3 types of implant materials currently used; metals, ceramics and polymers. A comparison of these biomaterials is summarized in Table 3.4. For instance, low back pain, osteoporosis and other musculoskeletal problems have been resolved by using permanent, temporary or biodegradable materials (Table 3.4). Total hip replacement has been the most successful orthopaedic procedure (Figure 3.2). The first successful prosthesis was made out of a Teflon acetabular cup with a stainless steel femoral component. The prosthesis was fixed to the bone using a cold curing polymethylmethacrylate (PMMA) polymer and is still widely used today in modified version [Wroblewski, 1999].

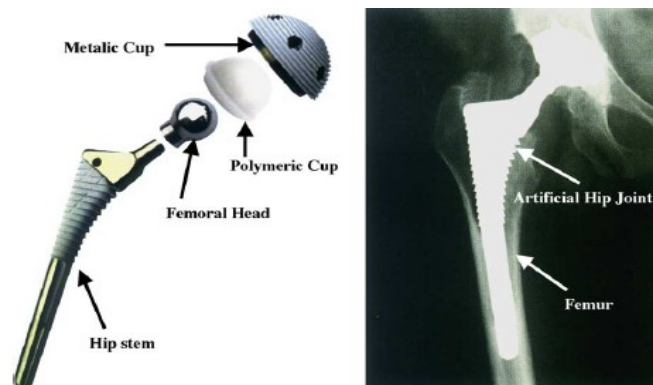


Figure 3.2: Implant for total hip replacement and bone screws and plates for fixation devices fixation [Liu *et al.* 2004].

Metals and alloys

The main groups of bio-metallic implants are stainless steel, cobalt alloys and titanium and titanium alloys. Although stainless steel has shown advantages as fixation devices due to its mechanical properties and corrosion resistance, it creates excessive stress-shielding of the bone as it is very stiff material [Ganesh *et al.* 2006]. It can also cause toxic reactions and dermatitis due to its high nickel content (10-14 wt %) [Karnerva 2001]. As for cobalt alloys, they are generally applied in orthopaedic prostheses for knee, shoulder and hip implants and possess excellent wear resistance for metal-on-metal load bearing surfaces in hip joints. Also, they are extremely hard and possess high corrosion resistance in body fluids. However, they have lower compatibility compared to titanium, poor fabricability and high cost, which make Co-based alloys unsuitable for biomedical applications [Marti 2000]. Titanium and its alloys, on the other hand, are the material of choice for biomedical applications due to their high strength-to-weight ratio and good fracture toughness which makes it ideal for load bearing applications. In addition, it has excellent corrosion resistance and biocompatibility compared to other metals [Ortrun, 2000]. Therefore, the development of porous metallic foam scaffolds for bone tissue ingrowth and drug delivery has been focused on titanium and its alloys [Li *et al.* 2002, 2006, 2007].

Polymers

PE has found applications as liner in acetabular cups, in total knee arthroplasties and as spacer in intervertebral disc replacement due to its combined increased strength, excellent toughness and biocompatibility [Fisher and Dowson 1991, Sutula *et al.* 1995]. However, despite their clinical success, several drawbacks have been reported with these types of polymers such as they release wear particles which induces inflammatory reaction [Maloney & Smith 1995].

Bioceramics

Bioceramics are one of the most extensively used synthetic materials. They are known for their exceptional wear rates, excellent corrosion resistance and high strength. [Murugan and Ramakrishna, 2004]. The first clinical application of bioceramics was introduced in 1970 to replace the traditionally used metallic femoral heads for hip prostheses with highly pure alumina [Boutin, 1972]. Orthopedic use of zirconia started in 1985 and showed higher fracture toughness than alumina. Both bioceramics have since been primarily used as femoral heads of total hip joints implants [Hulbert, 1993] due especially to its exceptionally low coefficient of friction and minimal wear rates. One of the earliest reports of hydroxyapatite-coated femoral stems in the body was by Furlong and Osborn [Furlong, 1991] followed by Geesink in 1986 [Geesink 1986]. Despite the fact that bioceramics are brittle materials, they have many advantages such as biocompatibility, non-toxic, non-immunogenic, readily available and easily formable.

3.9- Bone-Implant Interface

The reaction of the body to foreign materials, such as implants is different from normal healing. In essence, as described by Anderson in Figure 3.3, the first stage is the immediate adsorption of various types of non-specific proteins (i.e. fibronectin and vitronectin) onto the surface to control subsequent cell adhesion. It is important to note that previous studies have reported the osteoblasts preferentially adhere to specific amino acid sequences such as arginine-glycine-aspartic acid (RGD) [Balasundaram 2006]. Hence, presently, the development of new biomaterials is based primarily on altering the surface properties to overcome and control protein adsorption and cell attachment. There are two types of response after implantation. In cases where the implant is not biocompatible, macrophages adhere on the surface and fuse together to form giant cells which results into a fibrous avascular capsule around the material. This capsule prevents any proper biomechanical fixation and leads to implant failure. The second is the direct bone-implant contact without the intervention of a connective tissue layer, a process known in bone tissue as osseointegration.

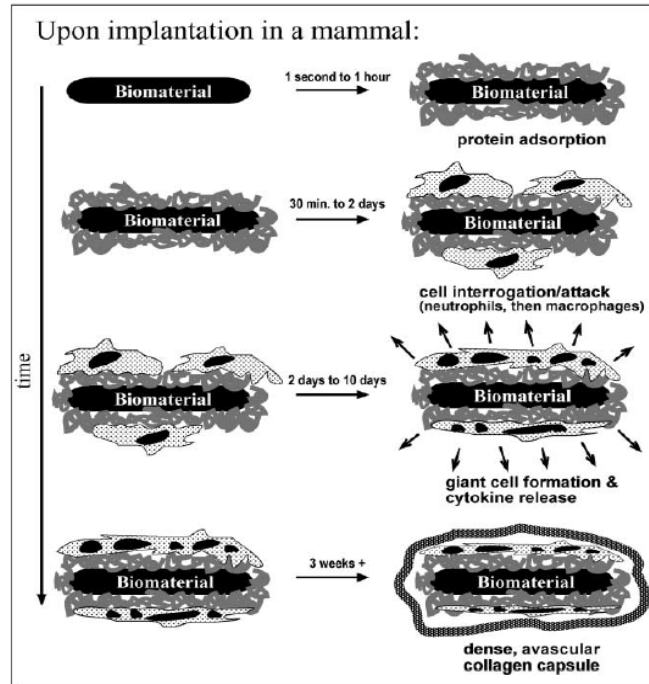


Figure 3.3: Steps involved upon implantation adapted by Anderson 1983.

3.9.1- Osseointegration

Osseointegration is defined as the direct contact between the bone and the material without the interference of a soft tissue. When a metal is implanted in the body, the first step of osteointegration is the migration and adherence of stem cells and osteoblast cells towards the implant. The composition of the matrix proteins is highly dependent on the metal surface. The last stage consists of tissue reorganization to become lamellar bone. It has been described in animal models that it takes at least 4-6 weeks for bone bone ingrowth in orthopaedic implants [Buser *et al.* 1991 and Takayuki 1997]. In humans however, it takes up to 3 months for osseointegration of prostheses to occur [Kim 1990]. It has also been reported that the transition from the formation of newly formed bone to stable lamellar bone arises between 18-24 months [Schenk 1995].

3.9.2-Types of Interface

Long term implant stability is determined to a great extent by the nature of the bone-implant interface.

Metal-Bone Interface

The first type of interface is the bone-implant interface. In order to improve implant stability, various modifications of metallic implant surfaces have been developed, ranging from the creation of macroscale porous metal surface to enable bone ingrowth and mechanical interlocking with the host tissue [Lueck *et al.* 1969], roughening of the surface such as by anodization, acid-etching and grit blasting [Le Guehennec *et al.* 2007] as well as by surface chemical treatments with NaOH [Mei Weia *et al.* 2002].

PMMA Cement-Bone

Another approach for improving fixation was the development of methyl methacrylate resins filled with PMMA beads, so called PMMA cements set by free radical polymerisation. However, numerous studies have shown that separation of the stem-cement interface and cracks *in situ* in the cement can precede clinical loosening of the implant [Jasty *et al.* 1990].

Ceramic-Bone

Various methods have been used to deposit HA coatings on metallic implants, such as plasma-spraying [Berndt 1990], laser deposition [Cotell *et al.* 1992] and electrophoretic deposition [Zhitomirsky *et al.* 1997] to name a few, to improve osteoconduction and bond strength. A comparison of these methods has been described by Yang *et al.* and is summarized in Table 3.5. This review will focus on plasma spraying and low temperature coatings since most techniques concerns these approaches.

Plasma Spray Coating

Among the vast array of coating processes, only plasma-spraying has gained commercial success [Berndt 1990, Clements *et al.* 1998 and Frayssinet *et al.* 1992] and has since been the most widely used method to coat metallic implants. The technique

involves the introduction of a flow of inert gas (i.e. Ar) between the water-cooled copper anode and the tungsten cathode (Figure 3.4). A direct current arc is then applied and the compressed gas is ionized and compressed to form an extremely high temperature plasma flame to help propel the material onto the substrate to be coated. This plasma temperature can reach up to 10 000K+. Therefore, any material that melts without decomposition or sublimation can be sprayed, as in the case of ceramic materials such as hydroxyapatite.

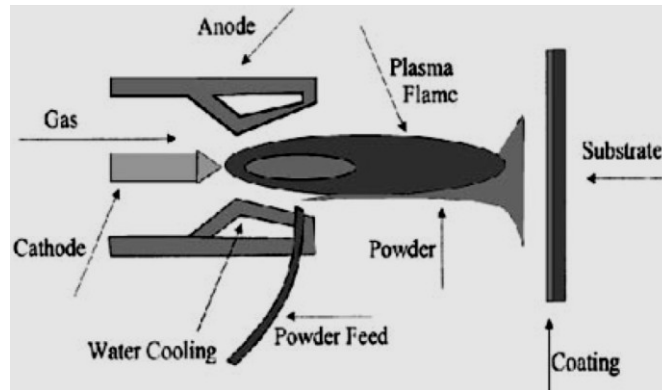


Figure 3.4: A schematic diagram of plasma spray deposition process [Narayanan 2007].

This method is currently widely used for depositing hydroxyapatite material on metallic implant surfaces. It is the most commonly used coating technique due to its fast and efficient deposition rate at a sufficiently low cost [Ong *et al.*, 1999 and Herman 1998]. However, this is a high temperature process which limits the application to thermally stable compounds and substrates. Needless to say, the incorporation of thermally unstable therapeutic compounds is unachievable. It has also been reported that plasma sprayed coatings can be delaminated and cracked when subjected to shear forces [Filiaggi *et al.*, 1991]. Also, because this is a “line-of-sight” process, it produces heterogeneous coatings on implants that have a complex 3D geometry (i.e. bone screws) [Kokubo 1996]. Kalita *et al.* demonstrated that the coating became more porous and rougher when the spraying angle was decreased from 90° to 50° [Kalita *et al.* 2005], area 1 to 3 (Figure 3.5).

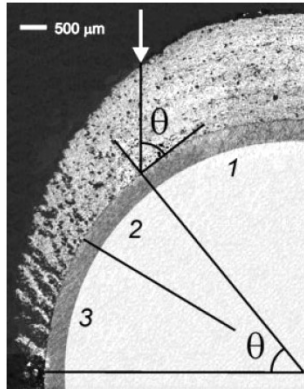


Figure 3.5: SEM micrograph of an uneven coating due to change in spraying angle. The arrow indicates the direction of the spray.

The disadvantages of plasma-coating techniques have shifted the attention onto other deposition processes such as ion-beam, sputtering and laser methods to produce thinner coatings. However, they are expensive and are most likely not commercially feasible, making them less attractive. Moreover, hot-isostatic pressing and thermal substrate techniques are unable to coat complex shapes. In spite of its many disadvantages, plasma-spraying remains the most commercially popular method.

Table 3.5: Different Techniques to deposit CaP/HA coatings (Yang *et al.* 1999)

Category	Method	Thickness	Advantages	Disadvantages
Low temperature process	Immersion in SBF	<30 μm	shape conformity	slow, requires replenishment and a constant SBF pH
	Other wet chemical methods	<30 μm	shape conformity , use of different Ca sources	
	Sol-gel method	<1 μm	shape conformity , thin coatings	controlled processing atmosphere, Expensive raw materials
	Cathodic deposition	0.2–90 μm	shape conformity, uniform coating, fast	Can produce poor adhesion, need control of electrolyte
	Electrophoresis	0.1–2 mm	Uniform thickness, fast, shape conformity	cracked coating, high sintering temp
High temperature process	Plasma spraying	30–200 μm	Fast, low cost	Decomposition, amorphous coating
	Ion-beam method	0.05–1 μm	High adhesion strength	Expensive, amorphous coating
	Laser method	0.1–5 μm	crystalline and amorphous phases, Dense and porous	Line-of- sight technique
	RF sputtering	0.5–3 μm	Uniform dense coating, dense coatings	Expensive, slow
	Hot-isostatic pressing	0.2–2 mm		Cannot coat complex shape, thermal expansion mismatch, elastic property difference
	Hydrothermal	0.2–20 μm	Crystalline phase, shape conformity	High pressure and temp

Low Temperature Coatings

Low temperature coating routes offer a promising alternative to high temperature processing techniques. Precipitation of hydroxyapatite on titanium implants using Kokubo's Simulate Body Fluid (SBF) has been the most commonly used [Feng *et al.* 2000, Habibovic *et al.* 2002, Barrere *et al.* 2006 and Bharati *et al.* 2005]. SBF synthetically replicates the inorganic ion concentrations found in human blood plasma [Kokubo and Takadama 2006]. A stable calcium phosphate coating requires that a chemical bond is formed between the metal and the calcium phosphate layer. The nucleation and formation of a calcium phosphate coating on titanium surfaces is usually achievable due to the presence of a passive oxide layer on the titanium implant (TiO_2), which makes the metal surface suitable for chemical reactions, usually the formation of calcium titanates. There are several factors that affect the coating formed such as exposure time, type of substrate, pre-treatment of the metal surface, over saturation, pH of the solution and the amount of crystal growth inhibitors [Chen *et al.* 2008]. The ability of low temperature formed calcium phosphates to incorporate proteins makes this technique of implant coating very convenient. For example, biomimetic carbonated hydroxyapatite coatings are able to incorporate antibiotics that can be used to prevent post-surgical infections [Stigter 2004]. However, calcium apatites are very insoluble, even supersaturated solutions do not contain sufficient ions to create an intact coating such that several solution changes are required [Habibovic *et al.* 2002].

Electrophoretic deposition (EPD)

Electrophoretic deposition involves the migration of colloidal particles suspended in a liquid medium under the influence of an electric field (electrophoresis) and is deposited onto an electrode, which is the metallic implant. All colloidal particles that can be used to form stable suspensions and that can carry a charge can be used in electrophoretic deposition. It is a low-cost, simple and flexible coating method for producing hydroxyapatite (HA) coatings on metal implants with a broad range of thicknesses. It allows for variation of the HA grain size and crystallinity by altering the cathodic potential and the pH of the electrolyte and concentration [Shirkhanzadeh and

Azadegan 1995]. The electrochemical deposition method to fabricate calcium phosphate coatings also uses aqueous electrolytes that contain Ca^{2+} and PO_4^- bearing ions solution such as SBF [Park *et al.* 2006]. However, this technique still suffers to get crack free and strong adhesive coatings.

Other low temperature coating processes, including sol-gel and cathodic deposition methods have also been explored. Although sol-gel offers stronger adhesion and cathodic technique provides a faster deposition rate, they are still highly dependent of the processing atmosphere or electrolyte [Young *et al.* 1999].

Despite their many advantages, low temperature deposition processes currently available never arrived at their full industrial potential as it is a relatively slow process (in the order of days) due to the very low solubility of apatite. Therefore, the source of anions and cations is limited and requires continuous replenishment of the solution [Narayanan 2008]. To overcome this problem, this work offers an alternative route to coat the surface by using the metallic surface as source of cations and react it with the anions containing solution to form calcium phosphate layer.

3.10- Calcium Phosphate

Historically, modification of titanium implants to render it osteoconductive was mainly focused on chemical and physical alteration of the surface. Eventually, further improvement of the osteoconductivity was achieved by depositing a bioactive calcium phosphate layer on the surface (i.e. HA and β -TCP are the most commonly used).

The calcium phosphate is released into the surrounding region of the implant and increases the saturation of the body fluid leading to the precipitation of biological active apatite on the material. This layer has shown to be essential to act as a bonding interface [de Groot *et al.* 1998, Daculsi *et al.* 2003]. It has been reported that bone cells (i.e. mesenchymal precursors and cells of the osteoblastic lineage) preferentially adhere, proliferate and differentiate into osteoblasts to form high-quality bone matrix on the apatite coating [Kokubo 1991]. Eventually, the surrounding bone tissue comes in contact with the apatite layer and forms a strong chemical bond [Hench 1991]. Many studies have reported that the biological fixation of titanium implants to bone is faster when

coated with calcium phosphate than without [Morris *et al.* 2000 and Barrere *et al.* 2003] and has better long-term clinical success [Geurs *et al.* 2002]. Promising approaches are also the incorporation of biological substances of the hydroxyapatite-coated titanium implants, using growth factor- β (TGF- β) family [Liu *et al.* 2006] and bone morphogenetic proteins (BMPs) [Liu *et al.* 2007, Hartwig *et al.* 2003 and Aebli *et al.* 2005].

For almost 30 years, interest has intensified in the use of calcium phosphates as biomaterials. However, only a selected few have been used as implants in the body since their solubility increases with decrease in Ca/P ratio (Table 3.6). In 1983, Driessens stated that calcium phosphates with Ca/P ratio of less than 1:1 were not suitable as implant materials. Other calcium phosphate compounds, such as brushite (DICP) ($\text{CaHPO}_4 \cdot 2\text{H}_2\text{O}$) and octacalcium phosphate (OCP) ($\text{Ca}_8\text{H}_2(\text{PO}_4)_6 \cdot 5\text{H}_2\text{O}$) have also been used but are not suitable for coating implants due to their fast resorption properties to the surrounding fluid in the body [Arifuzzaman and Rohani, 2004]. In increasing order, the relative solubility of the most relevant CaP compounds is as follow (Table 3.6); $\text{DCP} > \text{TTCP} > \alpha\text{-TCP} > \beta\text{-TCP} > \text{HA}$. The dissolution of HA coating increases with increase in porosity, surface area and a decrease in particle size and crystallinity [Legaros 1993 and 2002]. Calcium phosphate is used in several forms, ranging from granules, blocks and cements. A comparison of the advantages and disadvantages of the latter is summarized in Table 3.7.

Table 3.6: Properties of the biologically most relevant calcium orthophosphates with decrease in resorbability as compiled by [Dorozhkin 2008, Hagen 1975, Imas *et al.* 1996].

Compound	Formula	Ca/P molar ratio	Solubility at 37 °C (g /L)
Dicalcium phosphate	$\text{CaHPO}_4 \cdot 2\text{H}_2\text{O}$	1.0	0.227
Dicalcium phosphate anhydrous (DCPA), mineral monetite	CaHPO_4	1.0	0.122
α -Tricalcium phosphate (α -TCP)	$\alpha\text{-Ca}_3(\text{PO}_4)_2$	1.5	2.61×10^{-9}
β -Tricalcium phosphate (β -TCP)	$\beta\text{-Ca}_3(\text{PO}_4)_2$	1.5	4.78×10^{-11}
Tetracalcium phosphate (TTCP or TetCP), mineral hilgenstockite	$\text{Ca}_4(\text{PO}_4)_2\text{O}$	2.0	2.10×10^{-16}
Octacalcium phosphate (OCP)	$\text{Ca}_8(\text{HPO}_4)_2(\text{PO}_4)_4 \cdot 5\text{H}_2\text{O}$	1.33	2.20×10^{-39}
Hydroxyapatite (HA or OHAp)	$\text{Ca}_{10}(\text{PO}_4)_6(\text{OH})_2$	1.67	1.27×10^{-48}

Table 3.7. Comparison of different form of grafts; cement, granules and blocks.

Grafts	Advantages	Disadvantages	Notes and References
Cements	self-setting ability, good injectibility, osteoconductivity, moldability, biocompatibility, bioactivity, ease of preparation, low cost and can be used to deliver biomolecular compounds	lack of macroporosity, slow degradation <i>in vivo</i> , poor shear strength	Adapted from Dorozhkin, 2008
Granules	Easy to insert into preformed cavities, can easily be mixed with autogenous bone substitutes	requires a confined defect	[Liljensten <i>et al.</i> 2006]
Blocks	Formability, better control of porosity	no anatomical fit	

3.11- Magnesium and Magnesium Phosphate Biomaterials

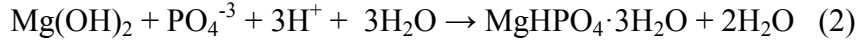
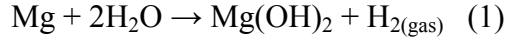
Another important class of bioceramics are the magnesium phosphates. There has been growing interest on this particular group of bioceramics due to their resorption properties which provide a temporary framework that dissolves as they are being replaced by the natural host tissue.

In 1907, pure magnesium to secure a bone fracture in the leg was the first degradable material implanted in the body [Lambotte 1932]. However, the implant corroded too quickly and generated hydrogen gas in the surrounding. Further attempts towards alloying the metal reported by Troitskii *et al.* and Znamenski *et al.* with cadmium and aluminum respectively, slightly improved the corrosion resistance of the material [Troitskii *et al.* 1944 and Znamenski *et al.* 1945]. However, for proper healing to occur, the implant is required to stay intact for at least +12 weeks [Witte *et al.* 2005]. These implants quickly corroded after only 1-2 months and subcutaneously generated a significant amount of hydrogen gas.

Therefore, several possibilities were used to tailor the corrosion rate of the material by using more complex alloying with rare earth (RE) elements and 2-10wt% aluminum [Witte *et al.* 2001, Stroganov *et al.* 1972 and Shaw 2003] and protective coatings by alkali heat-treatment [Grey and Luan 2002, Li 2004]. To date, the greatest success of magnesium based biomaterials are bioabsorbable coronary magnesium stents by *Biotronik*. It is composed of 93 wt.% Mg and 7 wt.% RE. Clinical trials among 63 patients resulted in no cardiac death or any medical complications after 4 months follow-up. The magnesium stents safely degraded after 2-3 months with no stent thrombosis. Future work in enhancing the corrosion resistance of this material is under development to be used as orthopaedic implants.

Promising outcomes of degradable magnesium based biomaterials has led this report to focus towards the magnesium phosphate class of bioceramics. In fact when magnesium corrodes in the body, it subsequently forms a more stable magnesium

phosphate compound which corrodes at a slower rate compared to pure magnesium or magnesium alloy. This can be explained by the following reactions of magnesium upon implantation in the body or immersion in a phosphate rich environment:



Magnesium phosphates have not only shown versatility in the biomedical field, but they are also the most researched and developed chemically bonded phosphate ceramics for multiple uses in many other applications. One of which is for the structural use of magnesium ammonium phosphate grout to quickly repair roads in cold conditions, industrial floors and airport runways [El-Jazairi 1982]. Other uses include the precipitation of struvite ((NH₄)MgPO₄·6H₂O) for the stabilization and solidification of radioactive and hazardous wastes and recycling of these benign products as agricultural fertilizers. It can also be found in the body as kidney stones, similar to newberyite (MgHPO₄·3H₂O). Biological occurrences of the crystal deposition of magnesium whitlockites (β-TCMP) have been found in cartilage sites from a study of 70 patients [Scotchford and Ali 1995], as primary component in dental calculi and predominantly abundant in calcified tissues. Other biological applications of this class of bioceramics are biodegradable cements for replacing hard tissue in the body [Waseleau *et al.* 2007]. Presently, *Bone Solutions Inc.*, is using a bio-absorbable and non-toxic magnesium based bone void filler as both injectable and mouldable material (*OsteocreteTM*) for dental and medical implants. Figure 3.8 below shows the solubility of different magnesium phosphates.

Table 3.8: Magnesium phosphate precipitation reactions in aqueous solutions with their respective solubility. [Wagh 2004].

Reactants	Products	Solubility at 37°C pK _{sp}
$\text{Mg}^{+2} + \text{HPO}_4^{-2} + 3\text{H}_2\text{O}$	$\text{MgHPO}_4 \cdot 3\text{H}_2\text{O}$	5.8
$3\text{Mg}^{+2} + 2\text{PO}_4^{-3} + \text{RH}_2\text{O}$	$\text{Mg}_3(\text{PO}_4)_2 \cdot 22\text{H}_2\text{O}$	23.1
“	$\text{Mg}_3(\text{PO}_4)_2$ (Amorphous)	15.9
“	$\text{Mg}_3(\text{PO}_4)_2 \cdot 8\text{H}_2\text{O}$	25.2
$\text{Mg}^{+2} + 2\text{OH}^{-1}$	$\text{Mg}(\text{OH})_2$	11.6

However, although extensive reports have been documented for their potential use as biomaterials, the mechanism behind their formation and cytotoxicity effects are still not well understood. The conditions that effect the formation of magnesium phosphates are important in order to determine the production of new magnesium phosphates, optimize their precipitation in both agro-industrial and waste water treatments, reduce their pathological occurrence in the body as well as explore their potential as new biomaterials.

References

Aebli N *et al.* Effects of bone morphogenetic protein-2 and hyaluronic acid on the osseointegration of hydroxyapatite-coated implants: an experimental study in sheep. J Biomed Mater Res A. 2005 Jun 1;73(3):295-302.

Aoki H. Science and medical application of hydroxyapatite. Japanese association of apatite science. 1991.

An YH and Draughn RA. Mechanical Testing of Bone and the Bone-Implant Interface. Published by CRC Press. 2000:41-64 and 133-145.

Arifuzzaman SM and Rohani S. Experimental study of brushite precipitation. Journal of Crystal Growth. 2004; 267: 624–634.

Ashley A *et al.*. Hydroxyapatite–Carbon Nanotube Composites for Biomedical Applications: A Review Int. J. Appl. Ceram. Technol. 2007;4(1):1–13.

Asavamongkolkul A *et al.* Stability of subchondral bone defect reconstruction at distal femur: comparison between polymethylmethacrylate alone and steinmann pin reinforcement of polymethylmethacrylate. J Med Assoc Thai. 2003; 86:626 -33.

Balasundaram G. A perspective on nanophase materials for orthopedic implant applications. Journals of Materials Chemistry. June 2006:3737-3745.

Barrere F *et al.* Osteointegration of biomimetic apatite coating applied onto dense and porous metal implants in femurs of goats. J Biomed Mater Res 2003;67:655–65.

Barrere F *et al.* Bone regeneration: molecular and cellular interactions with calcium phosphate ceramics. *International Journal of Nanomedicine* 2006;1(3) 317–332

Berndt CC *et al.* Spraying for bioceramic applications—A review. *Mater Forum*. 1990; 14:161–173.

Bharatis S *et al.* . Hydroxyapatite coating by biomimetic method on titanium alloy using concentrated SBF. *Bull. Mater. Sci.* © Indian Academy of Sciences. October 2005;20(6) 617–621.

Black J. *Orthopedic biomaterials in research and practice*. New York: Churchill Livingston. 1988:292-295.

Bohner M. Calcium orthophosphates in medicine: from ceramics to calcium phosphate cements. *Injury*. 2000;31:SD37–47.

Bonfield W. In: Hastings GW, Ducheyne P, editors. *Elasticity and viscoelasticity of cortical bone*. Boca Raton: CRC Press. 1984:43–60.

Boutin P. Total arthroplasty of the hip by fritted aluminum prosthesis. Experimental study and 1st clinical applications. *Rev. Chir. Orthop. Reparatrice Appar. Mot.*;1972;58, 229–246.

Buckwalter JA *et al.*. Bone biology. II: Formation, form, modeling, remodeling, and regulation of cell function. *Instr Course Lect*;1996;45:387–99.

Buser D *et al.* Influence of surface characteristics on bone integration of titanium implants. A histomorphometric study in miniature pigs. *J Biomed Mater Res* 1991;25:889–902.

Challis JH *et al.*. Strangulated lumbar hernia and volvulus following removal of iliac crest bone graft. *Acta Orthop. Scand.* 1975;46:230-233.

Chen X *et al.*. Effect of surface roughness of Ti, Zr, and TiZr on apatite precipitation from simulated body fluid. *Biotechnol Bioeng.* 2008;101(2):378-387.

Ciccone W *et al.* Bioabsorbable implants in orthopaedics: new developments and clinical. *J Am Acad Orthop Surg.* September/October 2001;9(5): 280-288.

Clements JAM *et al.* Healing of large (2 mm) gaps around calcium-phosphate coated bone implants: A study in goats with a follow-up of 6 months. *J Biomed Mater Res.* 1998; 40(3):341–349.

Coombes AG and Meikle MC. Resorbable synthetic polymers as replacements for bone graft. *Clin Mater.* 1994;17(1): 35–67.

Cornell CN and Lane JM. Current understanding of osteoconduction in bone regeneration. *Clin Orthop.* 1998;355(suppl):S267–273.

Cotell CM *et al.* Pulsed laser deposition of hydroxyapatite thin films on Ti-6Al-4V. *J Appl Biomater.* 1992;3(2):87–93.

Cowley S P and Anderson L D.. Hernias through donor sites for iliac-bone grafts. *J. Bone Jt. Surg.*:1983; 65A:1023-1025.

Daculsi G, Laboux O, Malard O, Weiss P. Current state of the art of biphasic calcium phosphate bioceramics. *J Mater Sci Mater Med.* 2003;14:195–200.

de Groot K, Wolke JG, Jansen JA. Calcium phosphate coatings for medical implants.

Proc Inst Mech Eng. 1998;212:137–47.

Dorozhkin S. Calcium orthophosphate cements for biomedical application. J Mater Sci.

2008; 43:3028–3057.

Ducheyne P. In vitro corrosion study of porous metal fibre coatings for bone ingrowth.

Biomaterials.1983;4:185–91.

Ellies LG *et al.*. Crystallographic changes in calcium phosphates during plasma-

spraying. Biomaterials. 1992;13:313–6.

Escalas F and DeWald RL. Combined traumatic arteriovenous fistula and ureteral injury:

a complication of iliac bone-grafting. J. Bone Jt. Surg..1977: 59A:270-271.

Evans FG and King A. In: Thomas CC, editor. Biomedical studies of the musculoskeletal

system. IL: Springfield.1961: 49–53.

Feder K. Orthopedic Biomaterials 2005 Report. Healthpoint Capital.

Filiaggi MJ *et al.*. Characterization of the interface in the plasma-sprayed HA coating/Ti-

6Al-4V implant system. J Biomed Mater Res 1991;25:1211–29.

Fisher J and Dowson D. Tribology of total artificial joints. Proc. Inst. Mech. Eng. J. Eng.

Med. 1991:205, 73–79.

Frayssinet P *et al.* New observations on middle term hydroxyapatite-coated titanium

alloy hip prosthesis. Biomaterials. 1992;13(10):668–674.

Furlong RJ and Osborn J F: Fixation of hip prostheses by hydroxyapatite ceramic coatings. J. Bone and Joint Surg. 1991;73-B(3):741-745.

Ganesh VK *et al.*. Biomechanics of bone-fracture fixation by stiffness-graded plates in comparison with stainless-steel plates. Biomed Eng Online. 2005;4:46.

Geesink, R. G.: Experimental and clinical experience with hydroxyapatite-coated hip implants. Orthopedics. 1989;12: 1239-1242.

Geurs NC, Jeffcoat RL, McGlumphy EA, Reddy MS, Jeffcoat MK. Influence of implant geometry and surface characteristics on progressive osseointegration. Int J Oral Maxillofac Implants 2002;17:811–5.

Gibbons DF. Materials for orthopaedic joint prostheses. In: Williams DF, ed. Biocompatibility of orthopaedic implants. Vol. 1 (CRC Series in Biocompatibility). Florida: CRC Press, Inc. 1982:112-95.

Grey JE, Luan B. Protective coatings on magnesium and its alloys—a critical review. J Alloys Compounds 2002;336:88–113.

Hagen AR. The stoichiometric solubility of calcium orthophosphates. Scand J Dent Res. 1975. 83(6):333-8.

Hench LL. Bioceramics: From concept to clinic. J Am Ceram Soc. 1991; 74(7):1487–1510.

Hench LL and Wilson J. Introduction to bioceramics. Singapore: World Scientific.1991.

Imas *et al.* Orthophosphate solubility in waters of different ionic composition. Fertilizer Research.1996. 44:73-78.

Jasty M *et al.*. Histomorphological studies of the long-term skeletal responses to well fixed cemented femoral components. J Bone Joint Surg. 1990;72A:1220–1229.

Kanerva L and Forstrom L. Allergic nickel and chromate hand dermatitis induced by orthopedic metal implant. Contact Derm 2001;44:103–4.

Kim YH and Kim VE. Uncemented porous-coated anatomical total hip replacement. J Bone Joint Surg 1990;72-A:45.

Kokubo T. 1991. Bioactive glass ceramics: Properties and applications. Biomaterials 12(2):155–163.

Kokubo T *et al.* Spontaneous formation of bone-like apatite layer on chemically treated titanium metals. J. Am. Ceram. Soc.1996;79:1127.

Kokubo T and Takadama H, Biomaterials. May 2006 :27(15) : 2907-2915.

Lambotte A. L'utilisation du magnesium comme materiel perdu dans l'osteosynthe`se. Bull Me´m Soc Nat Chir 1932;28:1325–34.

Lee NK et al. Endocrine Regulation of Energy Metabolism by the Skeleton. *Cell* . 2007;130: 456–469. doi:10.1016.

LeGeros RZ. Biodegradation and bioresorption of calcium phosphate ceramics. *Clin Mater*. 1993;14:65–88.

LeGeros RZ. Properties of osteoconductive biomaterials: calcium phosphates. *Clin Orthop Relat Res* 2002;395:81–98.

Le Gu'ehennec L et al. Surface treatments of titanium dental implants for rapid osseointegration. *Journal of Dental Materials*. 2007;23: 844–854.

Li JP *et al.*. Preparation and characterization of porous titanium. *Key Eng. Mater.*2002:.. 218–220, 51–54.

Li JP *et al.* Porous Ti6Al4V scaffold directly fabricating by rapid prototyping: preparation and in vitro experiment. *Biomaterials*. 2006: 27:1223–1235.

Li JP *et al.*. Bone ingrowth in porous titanium implants produced by 3D fiber deposition. *Biomaterials*.2007: 28: 2810–2820.

Li L *et al.*. Evaluation of cyto-toxicity and corrosion behaviour of alkali-heat-treated magnesium in simulated body fluid.*SurfCoat Technol*. 2004;185:92–8.

Li SM and McCarthy S. Further investigations on the hydrolytic degradation of poly(DL-lactide). *Biomaterials*. 1999;20, 35–44.

Liljensten E *et al.* Resorbable and Nonresorbable Hydroxyapatite Granules as Bone Graft Substitutes in Rabbit Cortical Defects.*Clinical Implant Dentistry and Related Research*. 2006;5(2): 95-102.

El-Jazairi, B., "Rapid Repair of Concrete Pavings," Concrete.1982;16(9): 12-15.

Elves MW and Salaman R. A study of the development of cytotoxic antibodies produced in recipients xenografts of iliac bone. J Bone Joint Surg.1974: 56B:331-339.

Feng QL *et al.* Influence of solution conditions on eposition of calcium phosphate on titanium by NaOH-treatment. Journal of Crystal Growth. 2000;210: 735-740.

Freeman *et al.* Freeman-Samuelson total arthroplasty of the knee. Clin Orthop 1985;192:46-58.

Gray's Anatomy: The Anatomical Basis of Medicine and Surgery, 40th edition (2008), 1576 pages, Churchill-Livingstone,Elsevier ISBN 978-0-443-06684-9;

Habibovic P *et al.*. Biomimetic Hydroxyapatite Coating on Metal Implants. J. Am. Ceram. Soc..2002: 85 (3) 517-22.

Hahn H and Palich W. Preliminary evaluation of porous metal surfaced titanium for orthopedic implants. J Biomed Mater Res 1970;4:571–7.

Harner CD *et al.* Allograft versus autograft anterior cruciate ligament reconstruction: 3- to 5-year outcome. Clin Orthop Relat Res (Clinical orthopaedics and related research) 1996 Mar(324): 134-44.

Hartwig CH *et al.*. Improved osseointegration of titanium implants of different surface characteristics by the use of bone morphogenetic protein (BMP-3): an animal study performed at the metaphyseal bone bed in dogs. Z Orthop Ihre Grenzgeb. 2003 Nov-Dec;141(6):705-11

Herman H. Plasma spraydeposition processes. MRS Bull 1988;12:60–7.

Hirschhorn J *et al.*. Porous titanium surgical implant materials. J Biomed Mater Res Symp 1971;2:49–67.

Hulbert SF. In: Hench LL, Wilson J, editors. An introduction to bioceramics. Singapore: World Scientific. 1993: 25–40.

Karagienes M. Porous metals as a hard tissue substitute. I. Biomedical aspects. Biomater Med Dev Artif Organs 1973:171–81.

Kim YH and Kim VE. Uncemented porous-coated anatomical total hip replacement. J Bone Joint Surg 1990;72-A:45.

Lidgren L. The Bone and Joint Decade-2000-2010. Bulletin of the World Health Organization. 2003; 81(9): 629-697.

Liu X *et al.*. Surface modification of titanium, titanium alloys, and related materials for biomedical applications. Materials Science and Engineering. 2004: 47(3-4)49-121.

Liu Y *et al.*. Incorporation of growth factors into medical devices via biomimetic coatings. Philos Transact A Math Phys Eng Sci. 2006 Jan 15;364(1838):233-48. Review.

Liu Y *et al.*. The influence of BMP-2 and its mode of delivery on the osteoconductivity of implant surfaces during the early phase of osseointegration. Biomaterials. 2007 Jun;28(16):2677-86. Epub 2007 Feb 12.

Lueck RA *et al.*: Development of an open pore metallic implant to permit attachment to bone. Surg Forum 1969; 20:456.

Maloney WJ and Smith RL. Periprosthetic osteolysis in total hip arthroplasty: the role of particulate debris. J. Bone Joint Surg. 1995;77A:1448–1461.

Marti A. Cobalt-base alloys used in bone surgery. Injury Int J Care Injured 2000;31:18–21.

Mei Weia *et al.*. Apatite-forming ability of CaO-containing titania, Biomaterials. 2002; 23 :167–172

Middleton JC and Tipton AJ. Synthetic biodegradable polymers as orthopedic devices. Biomaterials. 2000; 21: 2335–2346.

Miller SL and Gladstone JN. Graft selection in anterior cruciate ligament reconstruction. The Orthopedic clinics of North America. Oct 2002;33(4):675-683.

Morena R *et al.*. Fracture toughness of commercial dental porcelains. Dent Mater 1986;2:58-62.

Morris HF *et al.*. Periodontal-type measurements associated with hydroxyapatite-coated and non-HA-coated implants: uncovering to 36 months. Ann Periodontol 2000;5:56–67.

Murugan R and Ramakrishna S. Nanostructured biomaterials. In: Nalwa HS, editor. Encyclopedia of nanoscience and nanotechnology, California: American Scientific. 2004;7: 595–613.

Narayanan R *et al.*. Calcium phosphate-based coatings on titanium and its alloys. *J Biomed Mater Res B Appl Biomater.* 2008 Apr;85(1):279-99.

Ong JL and Chan CN. Hydroxyapatite and their use as coatings in dental implants: a review. *Crit Rev Biomed Eng* 1999;28:667–707.

Orban, JM *et al.*. Composition options for tissue-engineered bone, *Tissue Eng.* 2002, 8, 529-539.

Ortrun EMP. Unalloyed titanium alloys for implants in bone surgery. *Injury Int J Care Injured* 2000;31:7–13.

Pachence JM *et al.*. editors. Principles of tissue engineering. San Diego: Academic Press; 2000.

Park JH, Lee DY, Oh KT, Lee YK, Kim KM, Kim KN, *Materials Letters* 2006;60: 2573–2577, Bioactivity of calcium phosphate coatings prepared by electrodeposition in a modified simulated body fluid.

Parthiban JK, *et al.*. A radiological evaluation of allografts (ethylene oxide sterilized cadaver bone) and autografts in anterior cervical fusion. *Neurol India* 2002;50:17-22.

Phillips F M. Minimally invasive treatments of osteoporotic vertebral compression fractures, *Spine.* 2003: 28:S45–S53.

Rokkanen PU. Bioabsorbable fixation devices in orthopaedics and traumatology. *Ann. Chir. Gyn.* 1998;87:13–20.

Raab S *et al.* Thin film PMMA precoating for improved implant bone-cement fixation. *Journal of Biomedical Materials Research*, 1982;16:679-704.

Rubin JP and Yaremchuk MJ. Complications and toxicities of implantable biomaterials used in facial reconstructive and aesthetic surgery: a comprehensive review of the literature. *Plast. Reconstr. Surg.* 1997; 100:1336–1353.

Scotchford C, Ali Y. Magnesium whitlockite deposition in articular cartilage: a study of 80 specimens from 70 patients. *Annals of the Rheumatic Diseases* 1995; 54: 339-344.

Schenk R. Osseointegration von Sulmesh-beschichteten Press-fit-Pfannen. In: Schneider E, ed. *Biomechanik der Hüfte. Hefte zur Unfallheilkunde*. Berlin Heidelberg New York Stuttgart: Springer 1995.

Seiberling I. Osteoporosis a silent killer. *The Leader-Post*. November 2007.

Shaw BA. Corrosion resistance of magnesium alloys. In: Stephen D, editor. *ASM handbook volume 13a: corrosion: fundamentals, testing and protection*. UK: ASM Int.; 2003.

Shirkhanzadeh M and Azadegan M. Formation of carbonate patite on calcium phosphate coatings containing silver ions. *J. Mater. Sci Mater. Med.* 1998;9(7)385-391.

Simion M *et al.*. Vertical ridge augmentation using a membrane technique associated with osseointegrated implants. *Int J Periodontics Restorative Dent.* 1994;14:496-511.

Simske SJ *et al.* *Materials Science. Forum.* 1997;250:151.

M. Stigter *et al.* Incorporation of different antibiotics into carbonated hydroxyapatite coatings on titanium implants, release and antibiotic efficacy. *Journal of Controlled Release* 2004; 99(1):127-137,

St-Pierre *et al.*. Three-dimensional growth of differentiating MC3T3-E1 pre-osteoblasts on porous titanium scaffolds. *Biomaterials*. 2005; 26: 7319–7328.

Stroganov GB *et al.* Magnesium-base alloys for use in bone surgery. 1972. US Patent no. 3 687 135.

Stulberg SD. Design rationale and clinical results of a titanium porous coated total knee replacement. In Weinstein *et al.* *Uncemented Total Joint Replacement*, Phoenix, Harrington Arthritis Research Center. 1984:85.

Sutula LC *et al.* Impact of gamma sterilization on clinical performance of polyethylene in the hip. *Clin. Orthop.* 1995;319: 28–40.

Takayuki M *et al.* Cell and matrix reactions at titanium implants in surgically prepared rat tibiae. *Int J Maxillofac Implants* .1997;12:472–85.

Troitskii VV, Tsitrin DN. The resorbing metallic alloy ‘Osteosinthezit’ as material for fastening broken bone. *Khirurgiia* 1944;8:41–4.

Van Audekercke R and Martens M. In: Hastings GW, Ducheyne P, editors. *Mechanical properties of cancellous bone*. Boca Raton: CRC press; 1984: 89–98.

Kalita V and Gnedovets A. Plasma Spraying of Capillary Porous Coatings: Experiments, Modeling, and Biomedical Applications. *Plasma Process. Polym.* 2005;2:485–492.

Vert M. & Li SM. Bioresorbability of aliphatic polyesters. J. Mater. Sci. Mater. Med. 1992; 3:432–446.

Wagh A. Chemically bonded phosphate ceramics-21st Century Materials with Diverse Applications. Elsevier.

Waselau M *et al.* Effects of a magnesium adhesive cement on bone stability and healing following a metatarsal osteotomy in horses. American journal of veterinary research. 2007; 68(4):370-378.

Weber JN and White EW. Carbon-metal graded composites for permanent osseous attachment of non-porous metals. Mater Res Bull 1972;7(9):1005–16.

Wheeler KR *et al.*. Conf. Titanium Alloys in Surgical Implants. Philadelphia, USA: American Society for Testing and Materials, 1983. p. 241.

Witte F *et al.* In vivo corrosion of four magnesium alloys and the associated bone response. Biomaterials;2005;26(17):3557-63.

Witte F *et al.* Characterization of degradable magnesium alloys as orthopaedic implant material by synchrotron-radiation-based microtomography. 2001. http://www.hasylab.desy.de/science/annual_reports/2001_report/part1/contrib/47/5461.pdf.

Wroblewski BM *et al.* Charnley lowfrictional torque arthroplasty of the hip. 20 to 30 year results. J Bone Joint Surg Br 1999; 81:427-430.

Yaszemski MJ *et al.* Evolution of bone transplantation: molecular, cellular and tissue strategies to engineer human bone. Biomaterials .1996;17(2): 175–185.

Young JL *et al.* SEER's Web-based Training Modules. 2000.

Zhitomirsky I and Gal-Or L. Electrophoretic deposition of hydroxyapatite. *J Mater Sci Mater Med.* 1997; 8(4):213–219.^

Zimmermann, Michael (Frankfurt am Main, DE) Magnesium ammonium phosphate cement composition United States Patent 7115163

Znamenskii MS. Metallic osteosynthesis by means of an apparatus made of resorbing metal. *Khirurgiia* 1945;12:60–3.

Zreiqat H *et al.* The effect of surface chemistry modification of titanium alloy on signalling pathways in human osteoblasts *Biomaterials* 26 (36): 7579-7586, 2005.

CHAPTER 4: INVESTIGATION INTO AQUEOUS MAGNESIUM PHOSPHATE PRECIPITATION FOR BIOMEDICAL APPLICATIONS

Extensive studies have shown that magnesium phosphate such as newberyite and struvite can form at physiological conditions and have shown their efficacy in bone repair. However, little work is done behind the formation mechanism of magnesium phosphates and their biocompatibility with bone cells.

The study presented in this chapter aimed at investigating the precipitation conditions at which different phases of magnesium phosphates formed. This was achieved by varying the pH, temperature and concentration of the starting solutions. Characterization of the precipitates was performed using XRD, SEM, TEM, FT-IR, helium pycnometry, IEC and ICP. The effect of the magnesium phosphate precipitates on pre-osteoblast cells was assessed by cytotoxicity and cell viability tests.

Results from this study are being prepared for publications to Biomaterials and are reproduced with permission of co-authors.

4.1- ARTICLE 1

INVESTIGATION INTO AQUEOUS MAGNESIUM PHOSPHATE PRECIPITATION FOR BIOMEDICAL APPLICATIONS

Suzette Ibasco¹, Faleh Tamimi¹, Uwe Gbureck², Damien Le Nihouannen¹, David C. Bassett¹, Jonathan Knowles³, Adrian Wright⁴, Raymond Desjardins⁵, Srikar Vengallatore⁶, Edward Harvey⁷, Jake E. Barralet¹

¹Faculty of Dentistry, ⁶Department of Mechanical Engineering, ⁷Division of Orthopaedic Surgery, McGill University, Montreal (Canada), ²Department for Functional Materials in Medicine and Dentistry, University of Würzburg (Germany), ³ Eastman Dental Institute, University College London (United Kingdom), ⁴ School of Chemistry, University of Birmingham (United Kingdom), ⁵Terray Corporation, Arnprior, Ontario (Canada).

4.1.1- Abstract

Magnesium phosphates such as Newberyite ($\text{MgHPO}_4 \cdot 3\text{H}_2\text{O}$) are formed biologically and are known to be degradable and non toxic when implanted *in vivo*. Indeed, magnesium apatites have been shown to support osteoblast differentiation and function, and bone formation can occur around magnesium implants. However, very little is known regarding the precipitation and stability of magnesium phosphates in physiological environments. In order to address this, the formation of magnesium phosphate precipitates as a function of pH, temperature and ion concentration in aqueous solutions is reported. The precipitates were characterized by means of x-ray diffraction (XRD) scanning electron microscopy (SEM), Fourier transformation Infrared Spectroscopy (FTIR), inductively coupled plasma mass spectroscopy (ICP-MS), helium pycnometry and ion exchange chromatography (IEC). The precipitation conditions of

newberyite, amorphous tribasic magnesium phosphate hydrate, tribasic magnesium phosphate pentahydrate, holtedahlite, bobierrite and cattite were determined. Moreover, all the obtained magnesium phosphates proved to be biocompatible with osteoblast cultures and induced osteoblast adhesion and differentiation.

Keywords: Magnesium phosphate; Precipitation; Precipitates; Newberyite; Bobierrite; Cattite; Magnesium pentahydrate; Holtedahlite; Osteoblast; Cytotoxicity; Viability Assay; Amorphous magnesium phosphate; Magnesium phosphate crystals.

4.1.2- Introduction

Bioceramics have been dominated almost exclusively by studies of calcium phosphates, following attempts, for over 40 years, to develop synthetic, disease free and reproducible bone graft substitutes [1]. The two in any significant clinical use (tricalcium phosphate and hydroxyapatite), have limited proven advantageous biological properties namely osteoconduction and tissue bonding [1]. However, other salts are known to evoke these responses e.g. silicates and carbonates [2,3]. In addition to calcium, magnesium phosphates can occur in physiological and pathological mineralized tissues in the body. Whitlockite (β -TCMP) can be found in salivary gland stones, as well as in dental calculi [9], while struvite ($\text{MgNH}_4\text{PO}_4 \cdot 6\text{H}_2\text{O}$) and newberyite ($\text{MgHPO}_4 \cdot 3\text{H}_2\text{O}$) are found in kidney stones [10]. These materials have also been found to have good compatibility with bone tissue, and have shown their potential in the field of bioceramics and biomaterials for hard tissue regeneration [11]. Therefore, it is not surprising that one of the first degradable orthopaedic implants ever studied was a magnesium metal. Degradable magnesium alloys are currently being used as coronary stents, and are in magnesium phosphate cements under development for orthopaedic applications [4-6]. However despite the body of evidence surrounding their potential as biomaterials, there is very little information in the literature regarding their stability, precipitation conditions and cytotoxicity. To our knowledge, no previous study has been dedicated to explore the precipitation conditions of magnesium phosphates as a function of pH, temperature and

concentration of ions, and their compatibility with bone cells. This information is essential in order to optimize procedures for the production of new magnesium phosphate based materials, as well as for a better understanding of its stability under physiological.

Magnesium phosphate has been precipitated in different conditions, mainly by making stoichiometric mixtures of Mg:P of 3:2 to 1:1 in order to obtain neutral and acid magnesium phosphates for catalytic purposes [10]. However, the ratio of magnesium to phosphate ions *in vivo* is very different. For instance, magnesium concentration in serum is 0.7-0.9-mM, while phosphate concentration is 0.88-1.44 mM, leaving the ratio of Mg:P ~2:3 [11]. Despite their low concentration, magnesium phosphate salts can still form *in vivo* [12, 13]. Nevertheless, very little is known about the stability of these compounds in physiological conditions.

In this study, the crystalline regions of magnesium phosphate precipitates were mapped over a range of temperatures, pH and concentrations of the starting solutions. Moreover, the resulting materials were characterized, and their compatibility with osteoblast cell cultures was determined.

4.1.3- Materials and Methods

Precipitation

All reagent chemicals were purchased from Sigma Aldrich Inc.(St Louis, MO) and used without further purification.

In order to produce the precipitates, magnesium chloride and hydrogen phosphate solutions were mixed in a molar ratio of 2:3 Mg:P in order to obtain physiological [11] (0.67mM Mg^{+2} : 1.0 mM PO_4^{-3}), physiological x 10 (6.7mM Mg^{+2} : 10 mM PO_4^{-3}), and physiological x 100 (67mM Mg^{+2} : 100 mM PO_4^{-3}) concentrations. The temperature of the solutions was set at 4°, 21°, 37°, 55° and 75°C using a refrigerator (4°C), room temperature, water bath (37 and 55°C) and an oven (75°C); while the pH was adjusted prior to mixing with 1M H_3PO_4 and 1-10M NaOH. All solutions were buffered with tris-

(hydroxymethyl) aminomethane (0.1g per 1000ml). After initial mixing, the solutions were thoroughly stirred, and left to age for 24 hours at fixed temperature. The resulting precipitates were then centrifuged, washed in deionised water and were dried overnight in a vacuum oven at 37°C.

Characterization

X-ray diffraction (XRD) analysis of the precipitates was performed to evaluate their crystallographic nature. A vertical-goniometer X-ray diffractometer (Philips model PW1710, Bedrijven b. v. S&I, The Netherlands), X-ray diffraction (XRD), equipped with a Cu K α radiation source, was used for the powder diffraction pattern collection. Data were collected from 2 Θ of 10 to 80° with a step size of 0.02° and a normalized count time of 1 s per step. The phase composition was examined by means of the International Centre for Diffraction Data (ICDD) reference patterns.

The Fourier transform infrared spectroscopy (FT-IR) absorbance spectra of the precipitates were recorded (Nexus 470 Thermo-Nicolet, Thermo Fisher Scientific, Waltham, MA), having DTGS- KBr detector and KBr beam splitter with 32 scans at a resolution of 0.1 cm⁻¹. The spectrum of powdered sample in KBr medium was recorded in the range from 350 cm⁻¹ to 3000 cm⁻¹.

Characterization of the precipitates' morphology was performed using scanning electron microscopy (JEOL JSM- 840A SEM with an energy dispersive X-ray (EDX) detector, both operating at 200 keV).

Densities of the precipitates were measured using a helium pycnometer (Accupyc 1330; Micromeritics; Bedfordshire, UK) and their magnesium phosphate ratio was measured with inductively coupled plasma mass spectroscopy (ICP-MS). Samples (n = 3 per condition) were analyzed against Varian ICP-MS standard solutions (Merck, Darmstadt, Germany).

Solubility of the magnesium phosphate species was measured by detecting the Mg⁺² ion concentration at equilibrium in aqueous solution with an ion chromatography (Dionex co., Sunnyvale, CA).

Furthermore, cytotoxicity and bone biocompatibility of the magnesium phosphate powders was evaluated by measuring the lactate dehydrogenase (LDH) using a Cytotoxicity kit (Cytotoxicity Detection Kit^{Plus}, Roche applied Science, USA). Briefly, pre-osteoblastic cells (MC3T3-E1) (American Type Culture Collection, Rockville, USA) were seeded into 96-well plates with the magnesium phosphate precipitates, at a final density of 10^4 cells/well and incubated for 12h at 37°C in an atmosphere of 5% CO₂. MC3T3-E1 cells cultured on tissue culture-treated polystyrene (TP) brushite and plaster of Paris were used as the positive controls. Cells cultured with 2% Triton-X 100 lysis solution were used to measure the maximal LDH release. After 12 h, the medium was collected for LDH measurement and colorimetric measurement was performed on a spectrophotometer (FLUOstar OPTIMA, BMG Labtech, USA) with an optical density reading at 492 nm.

4.1.4- Results

Effect of solution concentration on magnesium phosphate precipitation:

The physiological solutions of magnesium phosphate were unable to form precipitates. However, the x10 and x100 concentrated physiological solutions formed precipitates at specific conditions (Figure 4.1).

Effect of pH and temperature on magnesium phosphate precipitation:

The XRD analysis of precipitates revealed the presence of different magnesium phosphates compounds depending on the reacting conditions (Figure 4.1). Figure 4.2 is a graphical summary of XRD analyses that revealed the different magnesium phosphate phases obtained under different temperatures, pH and concentrations. Below pH 6, no precipitates formed and at low temperatures (4-20°C) amorphous precipitates could also be found in solutions at pH 7.4 -10. Magnesium phosphates crystals formed mainly between pH 6 and 8 while at higher (pH 10-12), Brucite (Mg(OH)₂), was produced. Two groups of magnesium phosphate crystal were detected: the dibasic magnesium phosphate (DMP) at pH 6.0-7.4, and the tri-basic magnesium phosphates (TMP) at pH 7.4-10. Only

the tri-hydrated form of DMP (newberyite) was detected in all the different precipitates while 3 forms of hydrated TMP were detected depending mainly on the temperature. Cattiite ($\text{Mg}_3(\text{PO}_4)_2 \cdot 22\text{H}_2\text{O}$) was found to form at 4°C , bobierrite ($\text{Mg}_3(\text{PO})_2 \cdot 8\text{H}_2\text{O}$) at $4\text{-}20^\circ\text{C}$, and the pentahydrate form of TMP ($\text{Mg}_3(\text{PO})_2 \cdot 5\text{H}_2\text{O}$; TMPP) at $37\text{-}75^\circ\text{C}$. Unexpectedly, holtedahlite ($\text{Mg}_2\text{PO}_4\text{OH} \cdot 4\text{H}_2\text{O}$) was found to precipitate at 75°C and pH 7.4 together with bobierrite. However, when the starting solutions were diluted by an order of magnitude, the precipitation process render slower, and the precipitates shifted to form at higher pH and temperature. EDX analysis of the precipitates revealed that the composition of the precipitates prepared at pH below 10 was only magnesium phosphate and oxygen; while some sodium content was detected in precipitates obtain at alkaline pH 12 (not shown).

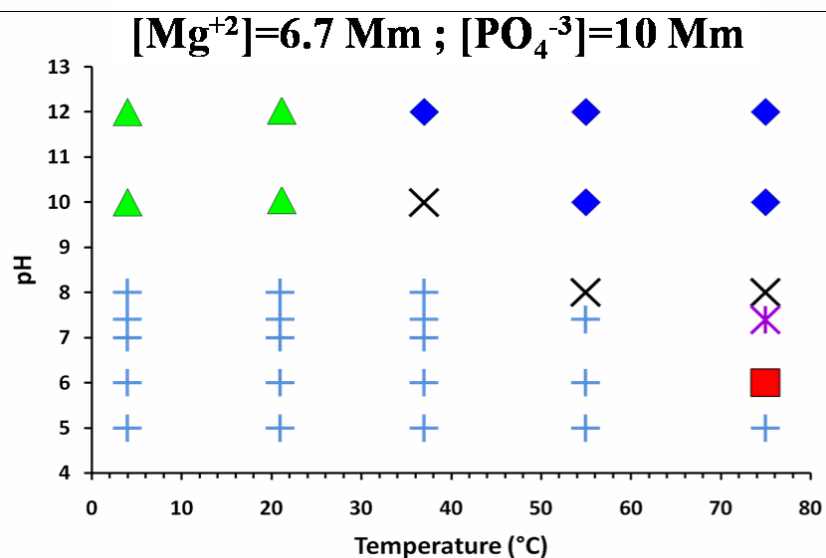
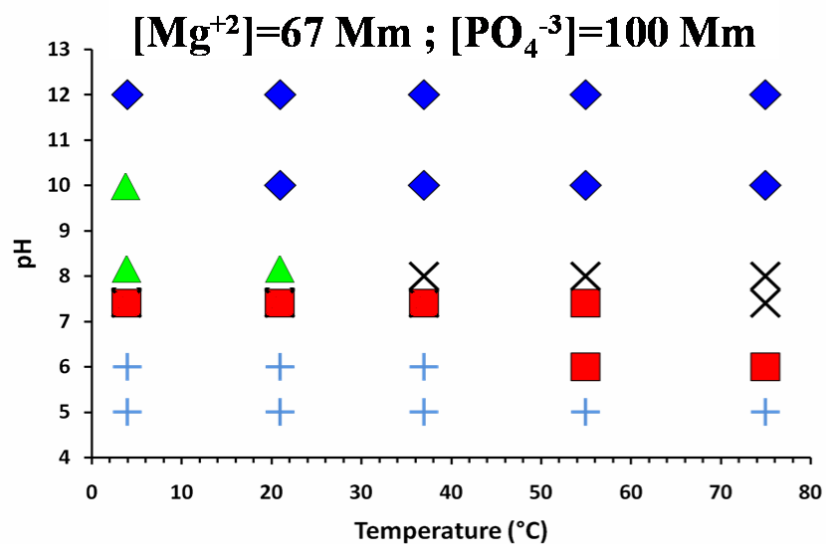


Figure 4.1: Magnesium phosphate precipitates as function of pH, temperature and concentration. Cattiite(▲); newberyite(■) magnesium hydroxide(◆);bobierrite and holtedahlite(*); TMPP(×); no precipitate (+).

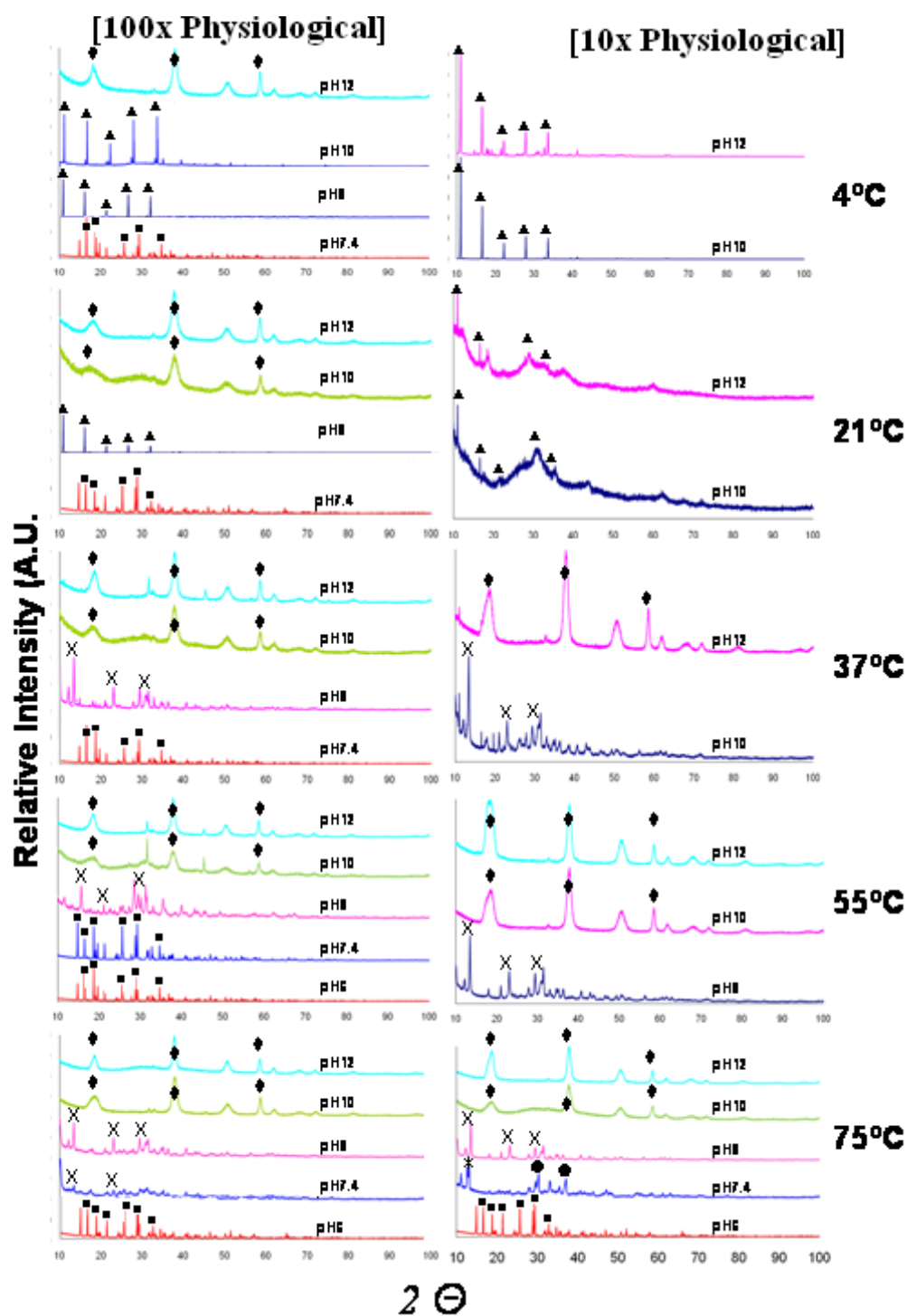


Figure 4.2: XRD of magnesium phosphate precipitates as function of pH, temperature and concentration. Cattiite(▲); newberyite(■) magnesium hydroxide(♦); bobierrite(*) ;holtedahlite (●); and TMPP(×).

FTIR spectra for the precipitates formed in concentrated conditions at different temperatures and pH are presented in Figure 4.3. The absorptions at 3545 cm^{-1} , 3490 cm^{-1} , 3284 cm^{-1} , 3168 cm^{-1} , due to intermolecular and weakly H bonded OH because of water of crystallization could be seen in the samples prepared at lower temperatures (4°C). Absorptions at 2375 cm^{-1} and 1722 cm^{-1} , as well as 577 cm^{-1} , 525 cm^{-1} and 665 cm^{-1} are due to the absorption of acid phosphates “(H-O-) P = O” and were present in samples precipitated at low pH [14]. The absorptions at 1061 cm^{-1} , 1217 cm^{-1} , and 1137 cm^{-1} are due to P = O associated stretching vibrations and seemed to be more pronounced at lower and intermediate pH samples (pH 7.4-10) and disappeared in samples prepared at higher pH. The 1648.86 cm^{-1} peak indicates the bent vibration of H–O–H in $\text{Mg}(\text{OH})_2$ containing samples prepared at pH 10-12.

The FTIR spectra confirmed the XRD analysis by revealing that precipitates containing hydrogen phosphates (newberyite) formed mainly at low pH values. Phosphates’ containing precipitates were formed at neutral pH (cattiite, bobierrite), while the precipitates formed at high pH had very little or no peaks at all related to phosphate groups, confirming the presence of magnesium hydroxide.

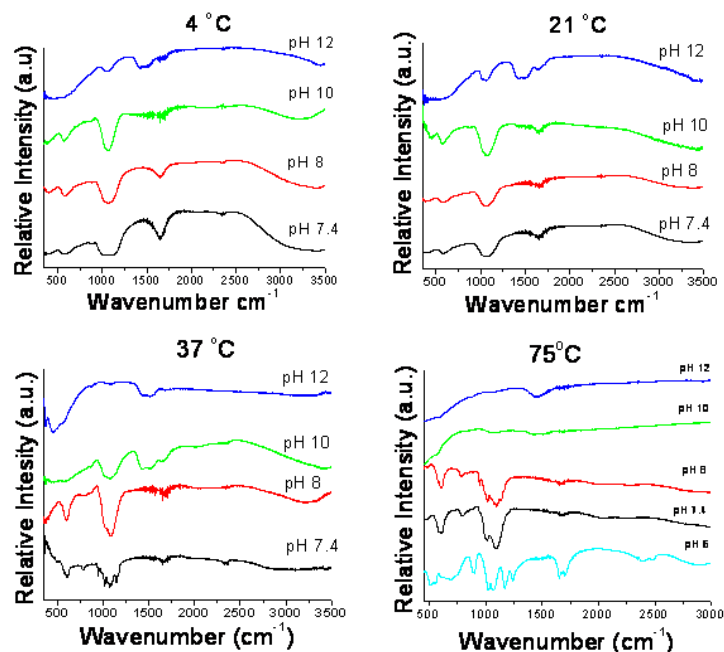


Figure 4.3: FTIR analysis of the precipitates obtained in concentrated solutions as a function of pH and temperature.

The crystal morphology of the obtained compounds was confirmed by SEM observations (Figure 4.4). Orthorhombic newberyite crystals, large triclinic crystals of Cattiite (4°C; pH 7.4), the parallel sheets of bobierite crystals formed at 75 °C pH 7.4, and TMPP at 37°C, pH 10 [15-18]. TEM micrograph and electron diffraction pattern of newberyite crystals can also be observed in Figure 4.6.

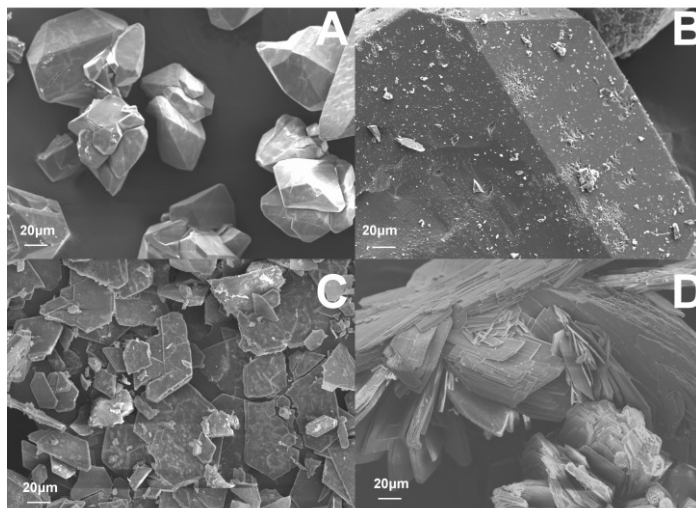


Figure 4.4: SEM pictures of the precipitates obtained at different conditions A: Newberyite (75°C; pH 6); B: TMPP (37°C; pH 10); C: Cattiite (4°C; pH 7.4); D: Bobierite (75°C; pH 7.4).

Effect of $[PO_4^{-3}]:[Mg^{+2}]$ on magnesium phosphate precipitation:

The effect of the P:Mg ratio was studied at physiological conditions (37°C; pH 7.4) maintaining a phosphate concentration in the solution of 100 mM. The XRD patterns and SEM observations revealed that the precipitates obtained with $[PO_4^{-3}]:[Mg^{+2}]=1.0-4.0$, were mainly Newberyite. However, at $[PO_4^{-3}]:[Mg^{+2}]$ of 4.0 and beyond, the material obtained was an amorphous phase of dibasic magnesium phosphate that eventually precipitated into small lamellar newberyite crystals (Figure 4.4B and 4.5).

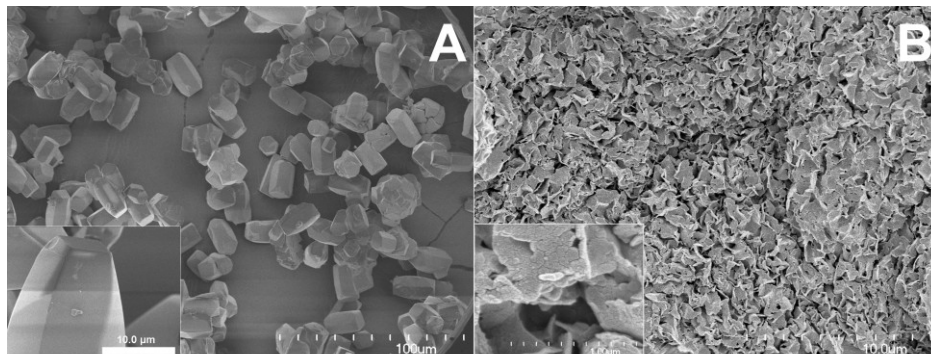


Figure 4.5: Characterization of precipitates obtained at different P:Mg ratios from solutions with a $[\text{PO}_4^{2-}] = 100 \text{ mM}$, at pH 7.4 and 37°C. A: SEM micrograph of precipitates obtained at $[\text{P:Mg}] = 1.0$. B: SEM micrographs of precipitates obtained at $\text{P:Mg} = 4.0$.

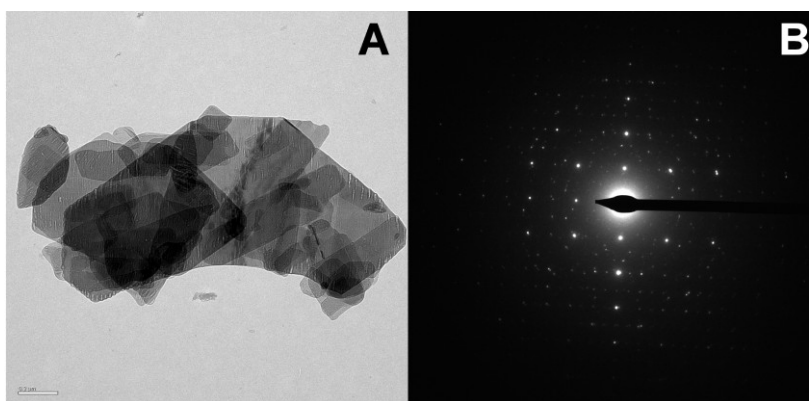


Figure 4.6: A: TEM micrograph; and B: TEM electron diffraction, of newberyite nanocrystals precipitated from solutions with a P:Mg ratio of 4; at pH 7.4 and 37 °C.

Physical chemical characterization of the obtained materials:

MS-ICP measurements of the precipitates showed the presence of three types of magnesium phosphates forming in aqueous solutions, the tetrabasic (holtedalite), tribasic (cattiite, bobierrite, TMPP), and dibasic magnesium phosphates. Unexpectedly, the amorphous phase obtained with high P:Mg ratios, had a dibasic magnesium phosphates composition (amorphous DMP). The measurement of the density of the samples matches those of the literature [15-19]. We report as well, for the first time, the density of the

amorphous DMP, and the TMPP (Table 4.1). The solubility of the different magnesium phosphate species lay within a reasonable range that allows their application as resorbable biomaterials (see Table 4.1).

Table 4.1: Density and ICP Measurements for samples prepared in concentrated solutions.

Compound	Mineral name	Solubility at 37°C		Precipitation conditions in this study		Density (g/cm ³)		Mg/P [15-19]		
		pK _{sp}	Ref	pH	Temperature	Experimental	Theoretical	Ref.	Experimental	Theoretical
MgHPO ₄ ·3H ₂ O	newberyite	5.8	[19,20]	6	55 °C	2.17±0.003	2.13	[16]	1.1±0.1	1.0
Mg ₃ (PO ₄) ₂ ·5H ₂ O	na*	17.7	This study	10	37 °C	2.36 ±0.24	na*	-	1.5±0.3	1.5
Mg ₃ (PO ₄) ₂ ·22H ₂ O	cattiite	23.1	[21]	7.4	4 °C	1.66 ±0.01	1.65	[17]	1.4±0.4	1.5
Mg(OH) ₂	brucite	16.8	[22]	12	37 °C	2.42 ±0.08	2.40	[22]	-	-

na: Not available *: The crystalline system of magnesium phosphate pentahydrate is unknown according to the 2008 update of PDF Ref code 00-035-0329.

In vitro assay of magnesium phosphate precipitates:

LDH cytotoxicity tests showed no significant differences between positive controls (tissue culture plastic) and cultures containing 10 mg of all the magnesium phosphates identified (see Figure 4.7).

The magnesium phosphate species precipitated at physiological conditions (newberyite and amorphous-DMP) was further studied for tissue engineering purposes. Upon visual, optical microscopy, SEM and observations, osteoblast adhesion, spreading and differentiation were obvious in both di-magnesium phosphates (Figure 4.7, 4.8 and 4.9). Osteoblast could spread and colonize these materials, showing their potential as tissue engineering scaffolds for bone repair.

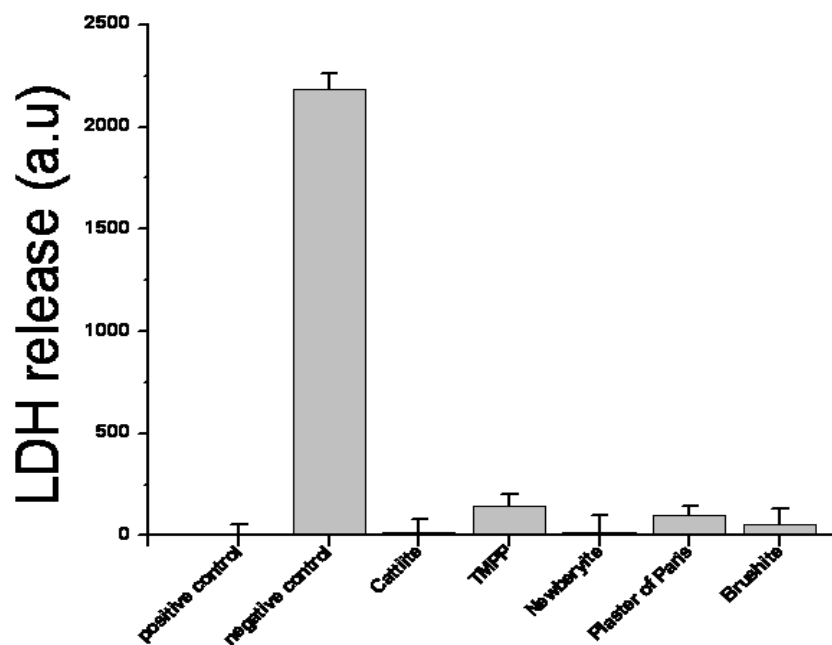


Figure 4.7: Graph of LDH cytotoxicity tests which revealed the magnesium phosphate powders to be non-toxic to pre-osteoblast cell line for 12h.

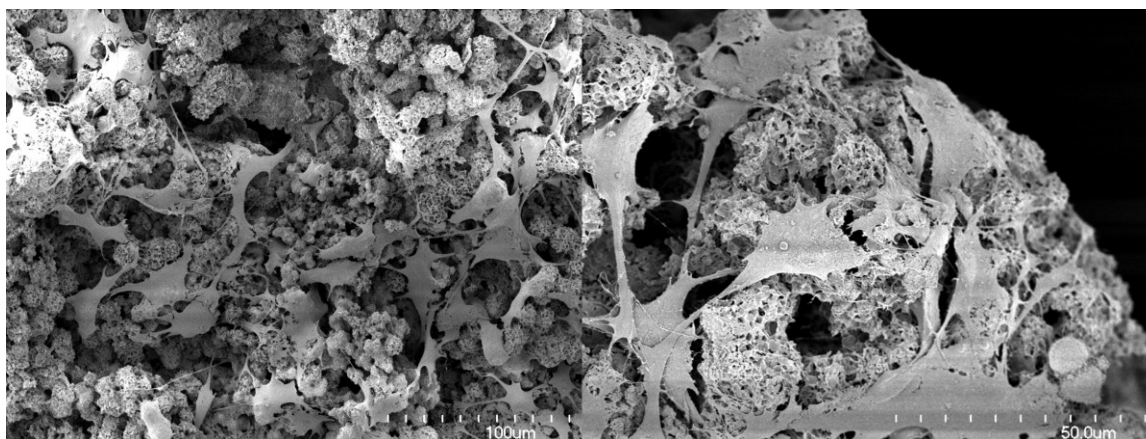


Figure 4.8: SEM micrographs of differentiated osteoblasts on newberyite (25mM[Mg⁺²]; 100 mM [PO₄⁻³] solution; pH 7.4; 21°C).

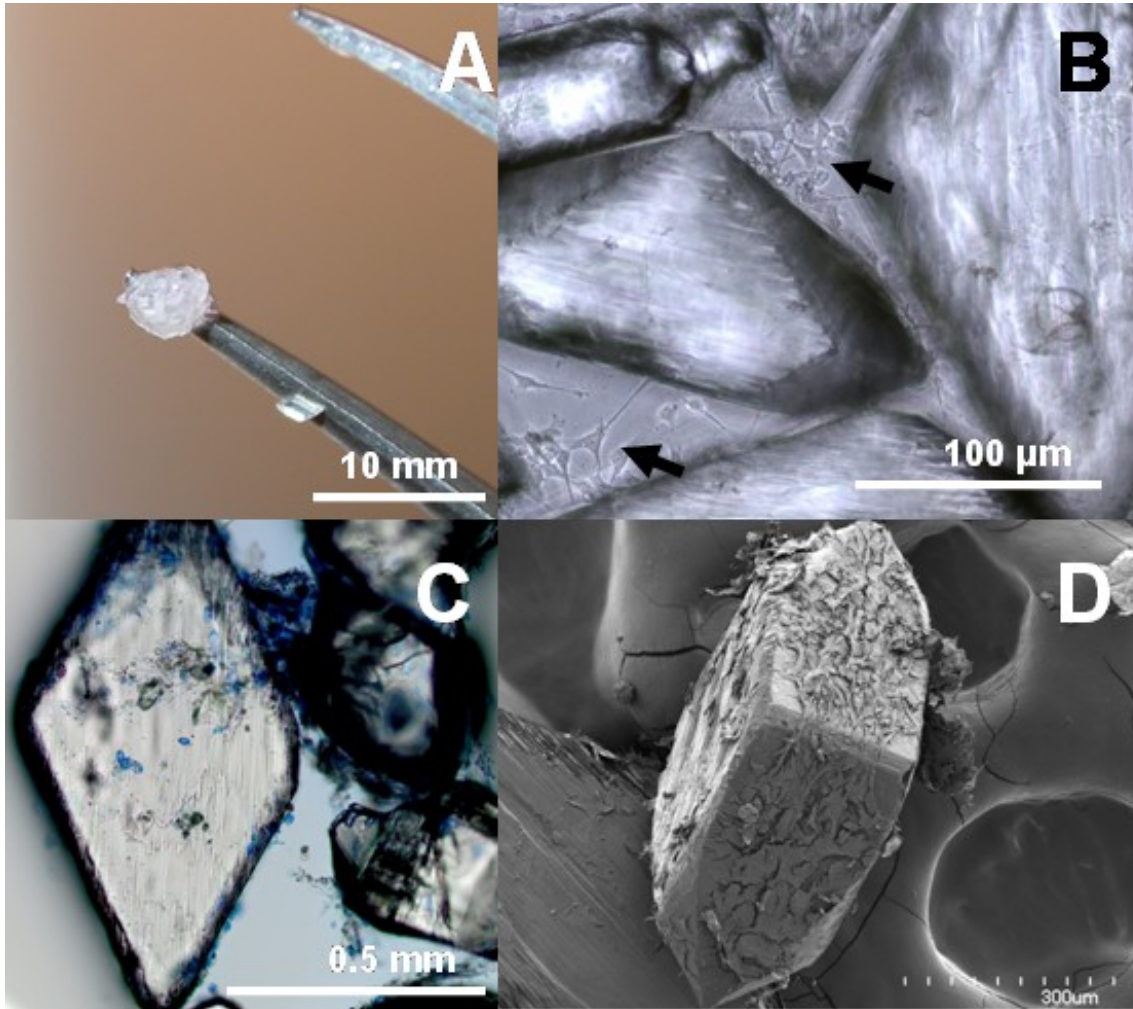


Figure 4.9: In vitro study of osteoblast cell culture on newberyite matrices prepared from a 67mM $[Mg^{+2}]$; 100mM $[PO_4^{-3}]$ solution; pH6; 55°C. A: Photograph showing cell mediated clustering of newberyite crystals. B: Optical micrograph graph showing osteoblast (Black arrows) adhering and attaching newberyite crystals together. C: Microscopic picture of osteoblast (stained with, methylene blue) colonizing the surface of newberyite. D: SEM micrographs showing the adhesion and spreading of osteoblasts over newberyite crystals.

4.1.5- Discussion

Magnesium ions chemistry is similar to that of calcium, and for this reason it is of special interest in the field of bioceramics as an adjuvant or substitutes of calcium based biomaterials [11, 23]. However, its smaller size gives in special features mainly in its capacity of interaction with water molecules. Calcium ion capacity to coordinate water molecules is lower than that of magnesium ions [24, 25]. For instance, tribasic calcium phosphates do not have structure water in both its α and β crystalline forms, while dibasic calcium phosphate is able to incorporate only two water molecules in its stable crystalline form (brushite) [26]. On the other hand, tribasic magnesium phosphates can incorporate up to 22 moles of crystallization water, while dibasic magnesium phosphates can incorporate up to 3 moles of crystallization water molecules depending on the precipitation conditions [10, 17].

Divalent magnesium is a "hard" ion that prefers binding to "hard" oxygen-containing ligands such as phosphates and water. The quite stable magnesium-water complexes usually possess octahedral symmetry in the first coordination shell [25]. At low energy states, magnesium ions in solution are able to interact with up to 18 water molecules simultaneously in a 2 sphere system in which the magnesium ion is in direct contact with 6 water molecules and in indirect contact with another 12 molecules present in the outer shield [27]. The free Gibbs energy needed to remove water molecules from the outer sphere is relatively low, that is why the magnesium phosphate precipitates that incorporated high amounts of water molecules in their crystalline structure were present only at lower temperatures (4-20°C). Indeed, cattite mineral has only been found in nature in extremely cold and humid natural environments [17]. With a mild increase in the energy of the system, magnesium ions shift from a two sphere into a one sphere system losing contact with all the external 12 water molecules [25, 27]. This explains why cattite and a-TMP formed at room temperature or below, while at higher temperatures (37-75°C) an abrupt reduction in the number water molecules incorporated in the precipitates to form TMPP and bobierite.

Moreover, the pH had an effect on the precipitating magnesium phosphate species, tri-magnesium phosphates occurred only above pH 7.4 regardless of the temperature, while magnesium hydrogen phosphates formed below pH 7.4. At pH 5.0, no precipitated form which seems to indicate probable formation of soluble mono-magnesium phosphate solutes. Hydrogen phosphate species were identified by FTIR only at low pH (below 7.4) favouring newberyite formation [14]. However, newberyite only precipitated with the higher concentration solutions due to its relatively high solubility at the pH levels tested in this study (see Table 4.1) [20].

The magnesium phosphate compounds identified seem promising for tissue engineering. This is because they were stable in physiological conditions, and were found to be biocompatible with osteoblast, similarly to other calcium phosphate and sulphates compounds that are currently being used as bone substitute biomaterials [1, 28]. Moreover, the fact that no magnesium precipitate was formed with the solutions containing physiological concentrations of magnesium to phosphate, as well as the solubility data, this seemed to indicate that the magnesium phosphates obtained in this study are likely to be resorbable *in vivo*, and therefore biodegradable.

4.1.6- Conclusion

The mapping of the crystalline and amorphous magnesium phosphate precipitates has been achieved by an aqueous precipitation method. It has been shown that the size, shape and type of magnesium phosphate compounds can be affected by control of the precipitation temperature, pH and concentration. This study reports new means under which this class of bioceramics form, which could be a useful model to investigate biocompatible coatings for metallic or polymeric implants used in biomedical applications. Several previously unevaluated magnesium phosphate phases would appear to have potential in orthopaedic applications and this warrants further study.

4.1.7- Acknowledgement

We acknowledge the financial support of an NSERC Strategic award, the FECYT grant (FT) and the Québec Ministère des Relations Internationales (Québec-Bavaria Exchange Program) PSR-SIIRI-029 IBI.

4.1.8-References

- [1] Dorozhkin S, Epple M. Biological and medical significance of calcium phosphates. *Angew Chem Int Edit* 2002;41(17): 3130-3146.
- [2] Saravanapavan P, Jones JR, Verrier S, Beilby R, Shirtliff VJ, Hench LL, Polak JM. Binary CaO-SiO₂ gel-glasses for biomedical applications. *Biomed Mater Eng*. 2004;14(4):467-86.
- [3] Combes C, Miao B, Bareille R, Rey C. Preparation, physical-chemical characterisation and cytocompatibility of calcium carbonate cements. *Biomaterials* 2006; 27(9): 1945-1954.
- [4] Erbel R, Di Mario C, Bartunek J, Bonnier J, de Bruyne B, Eberli FR, Erne P, Haude M, Heublein B, Horrigan M, Ilsley C, Bose D, Koolen J, Luscher TF, Weissman N, Waksman R. Temporary scaffolding of coronary arteries with bioabsorbable magnesium stents: a prospective, non-randomised multicentre trial. *Lancet* 2007;369(9576): 1869-1875.
- [5] Waselau M, Samii VF, Weisbrode SE, Litsky AS, Bertone AL. Effects of a magnesium adhesive cement on bone stability and healing following a metatarsal osteotomy in horses. *Am J Vet Res* 2007;68(4):370-8.
- [6] Wagh AS. Chemically bonded phosphate ceramics: 21st century materials with diverse applications. 1st eddition, 2004. Elsevier Science Ltd; Kidlington ,Oxford;UK. p 97-111.
- [7] Sugiyama S, Yokoyama M, Ishizuka H, Sotowa K, Tomida T, Shigemoto N.

Removal of aqueous ammonium with magnesium phosphates obtained from the ammonium-elimination of magnesium ammonium phosphate. *J Colloid Interface Sci* 2005;292(1):133-8..

[8] Qureshi A, Lo KV, Mavinic DS, Liao PH, Koch F, Kelly H. Dairy manure treatment, digestion and nutrient recovery as a phosphate fertilizer. *J Environ Sci Health B*. 2006;41(7):1221-35

[9] Burnstein LS, Boskey AL, Tannenbaum PJ, Posner AS, Mandel ID. The crystal chemistry of submandibular and parotid salivary gland stones. *J Oral Pathol* 1979;8(5):284-91.

[10] Miano R, Germani S, Vespasiani G. Stones and urinary tract infections. *Urol Int*. 2007;79 (1):32-6.

[11] Waselau M, Samii VE , Weisbrode SE , Litsky AS, Bertone AL. Effects of a magnesium adhesive cement on bone stability and healing following a metatarsal osteotomy in horses. *Am J Vet Res* 2007;68(4): 370-8.

[12] Petrov I, Soptrajanov B, Fuson N, Lawson JR. Infra-red investigation of dicalcium phosphates. *Spectrochim Acta* 1967;23(A): 2637-46.

[13] Boistelle R, Abbona F. Morphology, habit and growth of newberyite crystals. *Journal of Crystal Growth* 54 (1981) 275-295. North Holland Publishing Company.

[14] Ryu HS, Hong KS, Lee JK, Kim DJ, Lee JH, Chang BS, Lee DH, Lee CK, Chung SS. Magnesia-doped HA/beta-TCP ceramics and evaluation of their biocompatibility.

Biomaterials. 2004 Feb;25(3):393-401.

[15] Kim SR, Lee JH, Kim YT, Riu DH, Jung SJ, Lee YJ, Chung SC, Kim YH. Synthesis of Si, Mg substituted hydroxyapatites and their sintering behaviors. *Biomaterials*. 2003 Apr;24(8):1389-98.

[16] Takagi S , Mathew M, Brown WE . Crystal structures of bobierrite and synthetic $\text{Mg}_3(\text{PO}_4)_2 \cdot 8\text{H}_2\text{O}$. *Am Mineral* 1986;71: 1229-33.

- [17] Bartl H, Catti M, Joswig W, Ferraris G. Investigation of the Crystal Structure of Newberyite, $\text{MgHPO}_4 \cdot 3\text{H}_2\text{O}$, by Single Crystal Neutron Diffraction. *Tschermaks Min. Petr. Mitt.* 1983;32:187-194.
- [18] Britvin SN, Ferraris G, Ivaldi G., Bogadanova AN, Chukanov NV. Cattite, $\text{Mg}_3(\text{PO}_4)_2 \cdot 22\text{H}_2\text{O}$, a new mineral from Zhelezny Mine (Kovdor massif, Kola Peninsula, Russia). *N. Jb. Miner.*, 160-168 (2002)
- [19] Sutor D J. The crystal and molecular structure of newberyite, $\text{MgHPO}_4 \cdot 3\text{H}_2\text{O}$. *Acta Cryst* 1967; 23: 418-422.
- [20] Aramendía M A, Borau V, Jiménez C, Marinas J, Romero FJ. Synthesis and Characterization of Magnesium Phosphates and Their Catalytic Properties in the Conversion of 2-Hexanol. *Journal of Colloid and Interface Science* 1999;217(2): 288-98.
- [21] Abbona F, Lundager Madsen HE, Boistelle R. Crystallization of two magnesium phosphates, struvite and newberyite: Effect of pH and concentration. *J Cryst Growth*, 198; 57(1) 6-14.
- [22] Chickerur NS, Nayak GH, Lenka RC, Mahapatra PP. Solubility and thermodynamic data of magnesium hydrogen phosphate in aqueous media. *Thermochimica Acta*, 1982;58(1): 111-115.
- [23] Bhuiyan MIH, Mavrinic DS, Koch FA. Thermal decomposition of struvite and its phase transition. *Chemosphere* 2008;70: 1347–1356
- [24] Carl DR, Moision RM, Armentrout PB. Binding energies for the inner hydration shells of Ca^{2+} : An experimental and theoretical investigation of $\text{Ca}^{2+}(\text{H}_2\text{O})_x$ complexes ($x = 5-9$). *Int J Mass Spectrometry* 2007;265(2-3):308-25.
- [25] Markham GD, Glusker JP. The Arrangement of First- and Second-Sphere Water Molecules in Divalent Magnesium Complexes: Results from Molecular Orbital and Density Functional Theory and from Structural Crystallography. *J. Phys. Chem. B* 2002; 106: 5118-34.

[26] Tortet L., Gavarri J. R, Nihoul G., Dianoux A. J. Study of Protonic Mobility in $\text{CaHPO}_4 \cdot 2\text{H}_2\text{O}$ (Brushite) and CaHPO_4 (Monetite) by Infrared Spectroscopy and Neutron Scattering. *J Solid State Chem* 1997; 132(1): 6-16.

[27] Dzidic I, Kebarle P Hydration of the alkali ions in the gas phase. Enthalpies and entropies of reactions $\text{M}^+(\text{H}_2\text{O})_{n-1} + \text{H}_2\text{O} = \text{M}^+(\text{H}_2\text{O})_n$. *J. Phys. Chem* 1970; 74(7): 1466-74.

[28] Kebarle, P. Ion Thermochemistry and Solvation From Gas Phase Ion Equilibria. *Annu Rev Phys Chem.* 1977; 28: 445-76.

CHAPTER 5: REACTIVE MAGNESIUM SPUTTERED TITANIUM FOR THE FORMATION OF BIOACTIVE COATINGS

One major drawback of metallic implants is their inability to guide new bone formation and form a tight bond with surrounding bone. Several attempts have therefore been made to improve their osteoconductive and bone bonding properties.

The present chapter is a continuation of the previous study where magnesium phosphate, particularly struvite, is used to coat titanium implant. In parallel, we investigated a new low temperature technique to coat the metal by reacting sputter coated magnesium metal in different phosphate solutions. Magnesium containing coatings were achieved by varying the preparation conditions such as solution pH, temperature and concentration. The integrity of the coating was assessed by peel test, SEM microscopy and chemical analyses. The effect of the magnesium phosphate coating on osteoblast cells was also investigated by cytotoxicity and cell viability tests.

Results from this study have been submitted for peer review to Acta Biomaterialia and are reproduced with permission of co-authors.

5.1- ARTICLE 2

REACTIVE MAGNESIUM SPUTTERED TITANIUM FOR THE FORMATION OF BIOACTIVE COATINGS

Suzette Ibasco¹, Faleh Tamimi¹, Robert Meszaros², Damien Le Nihouannen¹, Srikar Vengallatore³, Edward Harvey⁴, Jake E. Barralet¹

¹Faculty of Dentistry, ³Department of Mechanical Engineering, ⁴Division of Orthopaedic Surgery, McGill University, Montreal (Canada), ²Department of Materials Engineering, University of Nürnberg (Germany).

5.1.1- Abstract

Osteoconductive coatings may improve the clinical performance of implanted metallic biomaterials. Several low temperature coating methods have been reported where a supersaturated solution is used to deposit typically apatitic materials. However, due to the very low solubility of apatite, the concentration of calcium and phosphate ions attainable in a supersaturated solution is relatively low (~1-2 mM), thus coating formation is slow with several solution changes required to form a uniform and clinically relevant coating. In order to avoid this problem, we present a novel method where substrates were initially sputter coated with pure magnesium metal and then immersed in differing phosphate solutions. In this method, upon immersion, the implant itself becomes the source of cations and only the anions to be incorporated into the coating are present in solution. These ions react rapidly forming a continuous coating and avoiding problems of premature non-localised precipitation. The resulting coatings from varying the phosphate solutions were then characterized in terms of morphology and composition by microscopy and chemical analyses. Upon immersion of the sputter coated metals into

ammonium phosphate solution, it was found that a uniform struvite ($\text{MgNH}_4\text{PO}_4 \cdot 6\text{H}_2\text{O}$) coating was formed. Upon subsequent immersion into a calcium phosphate solution, stable coatings were formed. The coated surfaces also enhanced both osteoblastic cellular adhesion and cell viability compared to bare titanium. The concept of sputter-coating a reactive metal to form an adherent inorganic metal coating appears promising in the field of developing rapid-forming low-temperature bioceramic coatings.

Keywords: titanium coating; magnesium sputtering; struvite; surface characterization; osteoblast.

5.1.2- Introduction

Metals have been the biomaterials of choice for biomedical load-bearing applications due to their combination of high mechanical strength and fracture toughness [1]. Hence, they are widely used as screws, plates, pins and implants (both orthopaedic and dental) where bone stabilisation and/or augmentation are required. The current types of metals used are cobalt chromium (molybdenum) alloys, stainless steel 316L, pure titanium and titanium alloys [2].

Despite sufficient mechanical strength, metallic biomaterials have limitations that can be clinically detrimental. For instance, the elastic modulus of currently used metals is much higher than that of natural bone which can create stress shielding effects [3]. This is typified by increased bone resorption around an implant as a disproportionate amount of the load is taken by the metal rather than the surrounding bone. Since the peri-implant bone undergoes resorption, the implant may loosen and eventually fail [3]. Additionally, metallic surfaces have a limited capacity to be integrated by bone, which is determined by features such as surface topography and chemistry and can release toxic ions through corrosion or mechanical wear [4, 5]. This can stimulate an inflammatory response and subsequently loss of bone which can lead to implant loosening [6, 7].

Certain coatings on metallic biomaterial surfaces have been shown to improve corrosion resistance and improve the bioactivity of the surface through osteoconduction i.e. bone ingrowth [8-10]. Several different coating approaches have been investigated to change the biological properties of metals and improve osteoconduction. These methods include plasma spraying of hydroxyapatite, alkali treatment of titanium surfaces to induce mineralization and direct precipitation of apatites in simulated body fluid [11, 12]. Plasma spraying is the most commonly used method for coating metals [13]. However, this is a high temperature process which limits the application to thermally stable coatings and substrates. Also, plasma-spraying does not allow for the coating of geometrically complex and porous surfaces [13]. Although aqueous deposition methods offer a solution to the limitations of plasma spraying, being a low temperature coating process and able to coat any exposed surface, the technique is time consuming and yet to be commercially realised [14, 15]. Alkali treatment of titanium [16, 17] has performed well *in vivo*, however the scope for varying surface and substrate chemistry is limited. Low temperature coating methods are very attractive since they allow the incorporation of thermally unstable biologically active compounds such as growth factors e.g. bone morphogenic proteins [18], adhesion molecules [19] and antibiotics [20] that may be used to improve the clinical performance of the metallic implant.

Traditionally, aqueous solution deposition of hydroxyapatite coatings is slow (in the order of days) [21]. This is due to the very low solubility of apatite such that the concentration of calcium and phosphate ions attainable in a supersaturated solution is relatively low (~1-2 mM). Therefore the solution's capacity to act as a simultaneous source of anions and cations is limited slowing the deposition rate and requiring continuous renewing of the solutions [21]. We sought to avoid this problem by providing a source of cations on the metallic surface with which to react and form a calcium phosphate layer. To achieve this, the metallic substrate was first sputter-coated with pure magnesium metal, then immersed in differing phosphate solutions to effectively 'pre-corrode' the magnesium before substituting the magnesium phosphate with calcium phosphate. Continuous coatings were formed rapidly therefore avoiding problems of premature non-localised precipitation.

Interestingly, magnesium phosphates may form pathologically in the human body and are found mainly in the form of struvite crystals ($\text{MgNH}_4\text{PO}_4 \cdot 6\text{H}_2\text{O}$) in kidney stones through the precipitation of trivalent phosphate in combination with ammonium ions [22-24]. Recent studies have exploited the biological importance of this mineral by suggesting a biodegradable and osteoconductive struvite based cement for bone regeneration procedures [25]. However, despite promising reports, the magnesium phosphates remain relatively unstudied as bioceramics. This study investigated the use of sputter coatings of pure magnesium metal on titanium substrates as a solid phase reactant for the production of inorganic bioactive coatings.

5.1.3- Materials and Methods

Magnesium sputtering of metallic substrates

Titanium sheet samples (6Al-4V alloy; 25.0 x 25.0 x 0.5 mm; McMaster-Carr Company, Los Angeles, CA, USA) were initially ultrasonically rinsed for 15 minutes in a 50/50 wt % ethanol/acetone solution. Without any further pre-treatment, the titanium alloy sheets were sputter coated with the Denton Explorer®-14 sputter coating system with a 3 μm thick magnesium layer using 99.5 wt % magnesium metallic targets (Goodfellow Cambridge Limited, England) of 20 cm diameter and a power of 150W in high purity argon.

Coating of Metals

In order to determine which solutions would be suitable for the formation of intact coatings, experiments were first performed by incubating the magnesium sputtered titanium sheets in simulated body fluid solution (SBF) [26], and in an SBF where potassium phosphate was substituted for sodium phosphate (Table 5.1). Next, SBF components were examined individually to determine which, if any, were capable of forming a coating. The four that formed a coating (as determined by scanning electron microscopy (JEOL JSM- 840A SEM with an energy dispersive X-ray (EDX) detector, both operating at 10-15 keV) were mixed in all permutations to examine the combinational effect on coating morphology, summarised in Table 5.1). The magnesium

sputtered samples were immersed in different precipitation solutions with a pH of 7.4 at 37°C for 24h (Table 5.1). In the case of struvite coatings magnesium coated samples were also immersed in ammonium diphosphate solution for 30 s, 2, 15 and 120 m, the reactions were arrested by immersing the samples in ethanol 100%, and were then vacuum dried before further characterization. Volumes (V_s ;ml) for the immersion liquid were calculated based on the formula: $V_s = S_a/10$

where S_a (cm^2) was the surface area of the sample as described previously [27] .

All coatings that were rapidly soluble in both phosphate buffered saline (PBS) and foetal bovine serum (FBS) were stabilised by immersion in a dilute calcium phosphate solution for 48h (Table 5.1). The non-sputtered reverse side of the titanium sheets was used as negative control.

Table 5.1. Composition and concentrations (mM) of the reacting solutions.

Sample ID Reactants	Modified SBF				SBF*	PBS	ADP	CaP
	A	B	C	D	E	F	G	H
KCl	0.225	0.225	-	0.225	0.225	2.68	-	-
$\text{Na}_2\text{HPO}_4 \cdot 7\text{H}_2\text{O}$	-	0.231	0.231	0.231	-	8.10	-	1.34
$\text{MgCl}_2 \cdot 6\text{H}_2\text{O}$	0.311	-	0.311	0.311	0.311	-	-	-
$\text{K}_2\text{HPO}_4 \cdot 3\text{H}_2\text{O}$	0.231	0.231	0.231	0.231	0.231	-	-	-
NaCl	-	-	-	-	8.035	136.89	-	-
KH_2PO_4	-	-	-	-	-	1.47	-	-
$\text{NH}_4\text{H}_2\text{PO}_4$	-	-	-	-	-	-	500	-
CaCl_2	-	-	-	-	0.292	-	-	2.00
NaHCO_3	-	-	-	-	0.355	-	-	-
Na_2SO_4	-	-	-	-	0.072	-	-	-

*SBF: Kokubo's SBF[26]; PBS: Phosphate Buffer Saline ; ADP: Ammonium Dihydrogen Phosphate ($\text{NH}_4\text{H}_2\text{PO}_4$); CaP: Calcium Phosphate

Characterization of the Coatings

All metal coatings were sputter coated with Au/Pd before being examined under scanning electron microscopy (SEM) coupled with an energy dispersion spectroscopy at a potential of 10 kV and a working distance of 12.0 mm to determine their morphology and elemental composition. X-ray diffraction (XRD) and atomic force microscopy (AFM) analysis of the coatings were performed to evaluate their crystallographic nature and topology. A vertical-goniometer X-ray diffractometer (Philips model PW1710, Bedrijven b. v. S&I, The Netherlands), equipped with a $\text{Cu K}\alpha$ radiation source, was used for the powder diffraction pattern collection. Data were collected across a 2θ range of 10 to 80° with a step size of 0.02° and a normalized count time of 1 second per step. The phase composition was examined by means of the International Centre for Diffraction Data (ICDD) reference patterns. An AFM (MFP-3D-BIO/Olympus IX71; Asylum Research, Santa Barbara, CA) in non contact mode was used to make high definition topographical images of the dry surfaces of the samples at room temperature.

In order to investigate coating thickness and homogeneity, coated metals were embedded in a resin mounting medium (Technovit 2000 LC, Heraeus Kulzer GmbH, Wehrheim Germany). The samples were then cut and ground through the metal coating with a silicon carbide grinding sequence (600, 800, 1200 and 2400 grits), followed by polishing with a fine alumina slurry on a medium nap cloth an examination under SEM.

Durability of the coating was assessed using a peel test [27]. To test the stability of the coatings under physiological conditions, coated samples were immersed in phosphate buffer solution (PBS) and Foetal Bovine Serum (FBS) for 24h at 37°C and samples were examined by SEM and AFM.

Osteoblast cell culture

The murine pre-osteoblastic cell line MC3T3-E1 was obtained from the American Type Culture Collection (ATCC, Rockville, USA). MC3T3-E1 cells were cultured in 25 cm² tissue culture flasks in MEM culture medium with 10 % FBS, 1 % L-glutamine, 1 % penicillin/streptomycin and 1 % sodium pyruvate at 37 °C in a humidified atmosphere containing 5 % CO₂ in air. Cells were sub-cultured once a week using trypsin/EDTA and maintained at 37 °C in a humidified atmosphere of 5% CO₂ in air. The medium was renewed every 2 days.

Cell adhesion

The MC3T3-E1 cell adhesion was quantified on bare titanium (T) and calcium phosphate coated titanium (CT) square materials (1 cm²). Cells were seeded onto the surface of T, and CT in 24-multiwell plates at a final density of 2.0×10^6 cells/cm². After 2 hours, non-adherent cells were removed from the material surface by vortexing the samples in fresh culture medium for one minute. The attached cells were determined by cell counting using a hemocytometer following cell detachment by treatment with a trypsin-EDTA solution (0.05%). Experiments were performed in triplicate.

Cell viability

The viability of pre-osteoblastic cells was determined by the Live/Dead[®] Viability/Cytotoxicity Kit (Molecular Probes, Eugene, OR, USA). The Live/Dead[®] Viability/Cytotoxicity Assay Kit provides a two-color fluorescence cell viability assay which is based on the simultaneous determination of live and dead cells by detection of the intracellular esterase activity by calcein AM and of plasma membrane integrity by ethidium homodimer (EthD-1), respectively. Cells were washed three times with sterile PBS and incubated for 30 min at room temperature in 20 µl of PBS solution containing 2 µM calcein-AM and 4 µM EthD-1. The samples were then examined under a fluorescence microscope (Eclipse TE 2000-U, Nikon Instruments Inc., Melville, NY, USA) (x4). The percentage of viable cells was determined by scanning five randomly chosen fields from each slide, with at least 100 cells being analyzed per field.

5.1.4- Results

SEM examination revealed that aqueous solutions containing either KCl, $\text{Na}_2\text{HPO}_4 \cdot 7\text{H}_2\text{O}$, $\text{MgCl}_2 \cdot 6\text{H}_2\text{O}$, K_2HPO_4 , or $\text{NH}_4\text{H}_2\text{PO}_4$ as single components, reacted with the magnesium layer to form stable phosphate precipitates, while no precipitates were formed on the non-sputtered side of the titanium sheets. Although precipitates did form when immersed in these single component solutions and two component combinations of the same salts, the coating was patchy at a microscopic level (not shown). Three component combinations, as shown in Table 5.1, were slightly better (Figure 5.1; Sample A-C), and a uniformly cracked magnesium phosphate coating was apparent when combining all 4 active components (Figure 5.1; Sample D). It was also determined by EDX analysis that agglomerated precipitates of magnesium phosphate and magnesium chloride could be achieved in immersing solutions containing phosphate and chloride ions. Immersion in both non modified SBF solution (Figure 5.1; Sample E) and PBS solution showed that although a coating of magnesium phosphate was formed, it was irregular in morphology and cracked in places (Figure 5.1; Sample F).

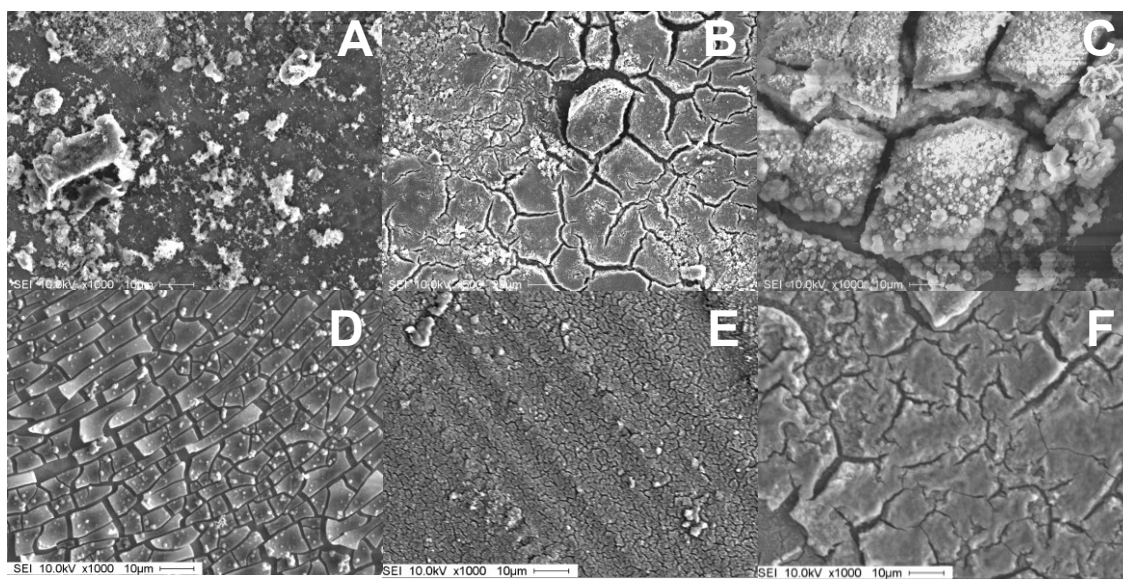


Figure 5.1: A-C) SEM images of magnesium coated metals immersed in 3 component combinations, D) 4 component combination E) SBF and F) PBS .

Following immersion in ammonium diphosphate solution (ADP), struvite crystals rapidly formed over the surface within few seconds, to be fully coated in just 2 minutes (Figure 5.2). After 24h of immersion in ADP, the dense and uniform coating of struvite appeared to be stable without any apparent cracks (Figures 5.2, 5.3A,). The struvite crystals appeared to radiate from a central nucleus forming circular polygonal microscale domains across the surface (Figure 5.3A).

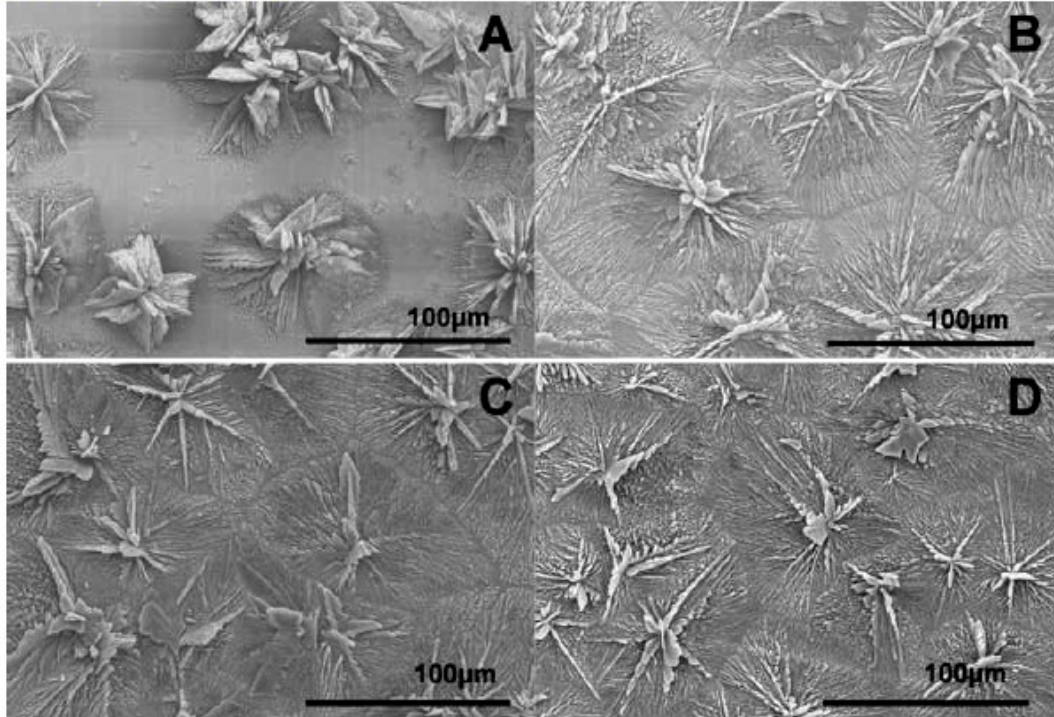


Figure 5.2: SEM micrographs of Mg sputtered titanium sheets after immersion in ADP solutions for periods of 30 seconds (A); 2 minutes (B); 15 minutes (C); and 2 hours (D).

Linear EDX of the coating cross section, as well as the XRD, revealed that a small amount of magnesium remained unreacted below the struvite coating adhered to the titanium surface (Figure 5.3E).

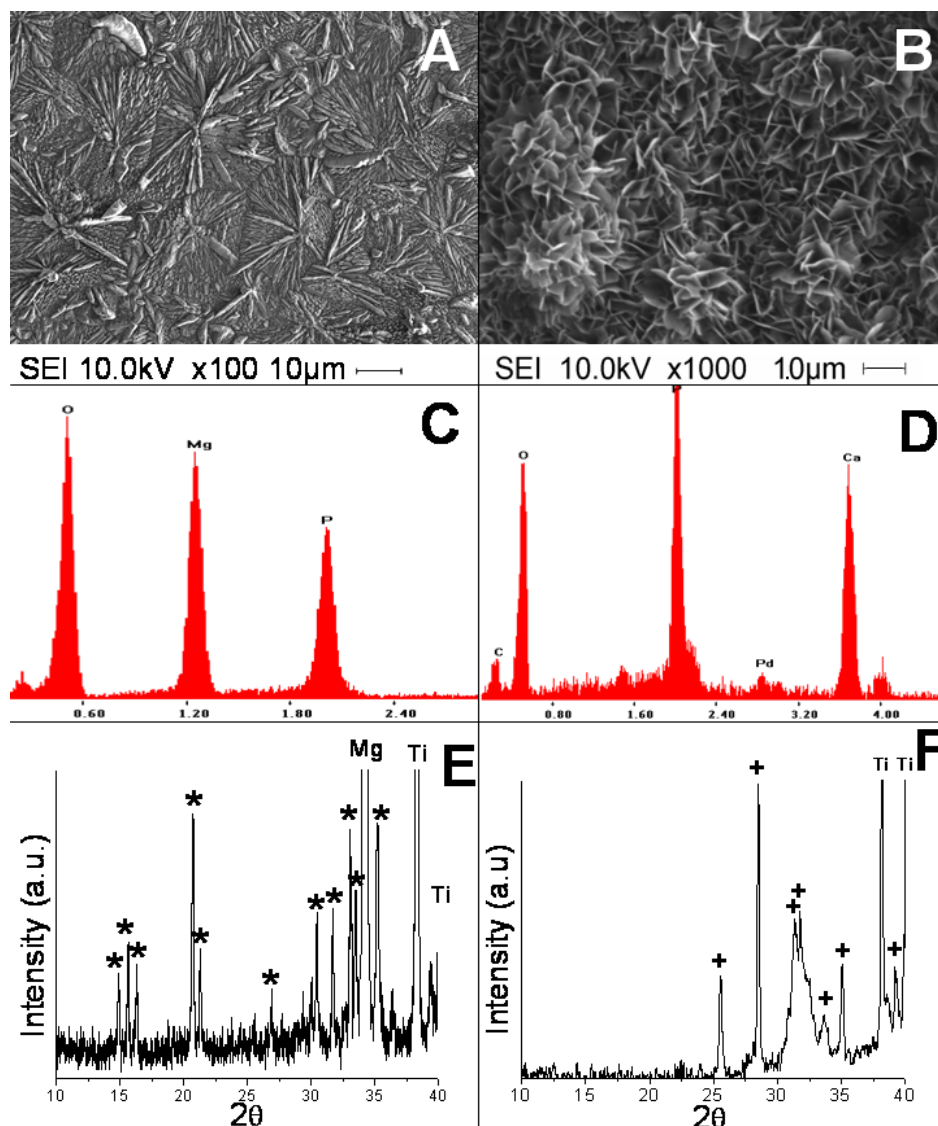


Figure 5.3: SEM, EDX and XRD analysis of (A,C,E) struvite coated sample before and (B,D,F) after additional coating with calcium phosphate solution. (*) indicate struvite peaks diffraction peaks (+) indicate hydroxyapatite peaks.

Interestingly, linear EDX analysis of the coating cross section revealed small amounts of magnesium and oxygen between the external struvite layer (Figure 5.4) and the inner unreacted Mg, this could correspond to an intermediate layer of magnesium hydroxide. When compared to magnesium sputtered metals immersed in CaP solution, no coatings were achieved, only bare metal. Post-treatment of the struvite coating in a

CaP solution showed a uniform array of calcium phosphate platelet crystals and formed a crack free surface (Figure 5.3B). EDX line scan analysis of the cross section indicated the thickness of the calcium phosphate layer to be $\sim 10\ \mu\text{m}$ (Figure 5.4). Linear EDX confirms XRD analysis by revealing that the coating composition is of calcium phosphate (Figure 5.4).

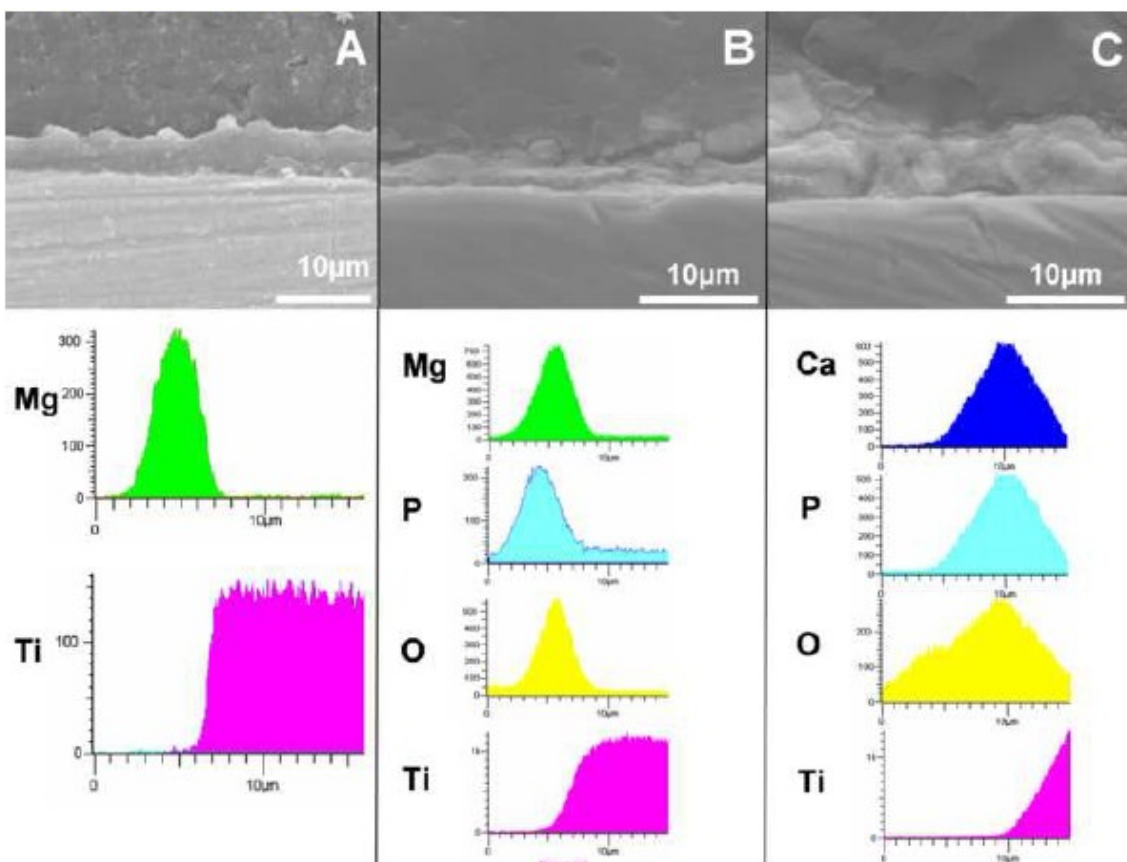


Figure 5.4: SEM micrographs and linear EDX analysis of the sample cross section for: A) Mg sputtered coated titanium; B) struvite coated titanium; and C) HA coated titanium.

EDX analyses revealed that the coatings formed on samples A-F, were thin and/or cracked as strong peaks for the metal substrate were found even at low beam current (data not shown). However, EDX analysis of the struvite coating (Figure 5.3C) confirmed the presence of a thick uniform magnesium phosphate coating, furthermore, the

composition of this coating changed into calcium phosphate when immersed in CaP solution (Figure 5.2D).

XRD analysis confirmed the presence of struvite in the samples incubated in ADP solution, residual unreacted magnesium metal was also detected (Figure 5.3E; Sample G). XRD patterns of struvite coatings after the secondary coating in CaP solution revealed peaks characteristic of hydroxyapatite and no magnesium metal was detected (Figure 5.3F).

Precipitated struvite formed block shaped microcrystals with heights up to $\sim 2 \mu\text{m}$ that were imaged using AFM (Figure 5.5A). Upon immersion in a calcium phosphate solution the struvite microcrystals were replaced with thin (100-200 nm) plate-like crystals up to $2.5 \mu\text{m}$ in height and between 2 and $4 \mu\text{m}$ in length (Figure 5.5B).

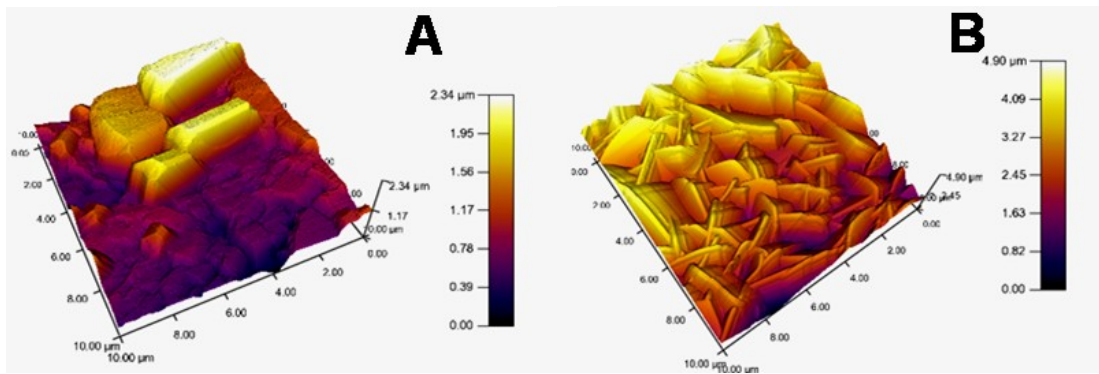


Figure 5.5: A) AFM images of the struvite crystals and B) the calcium phosphate platelet crystals secondary coating.

The struvite and CaP coatings were durable enough to withstand the peel test as determined by SEM examination before and after the test (not shown). Attachment of pre-osteoblasts on the CaP coating showed enhanced attachment compared with the bare titanium surface. SEM observations revealed osteoblast adherence on the coated surfaces (Figure 5.6; A and B). Cell survival and adhesion was significantly enhanced as well with CaP coated titanium (Figure 5.6; C and D), after 8 days culture the survival rate was 70-80% compared with 1% after 4 days culture on uncoated titanium alloy (Figure 5.6D).

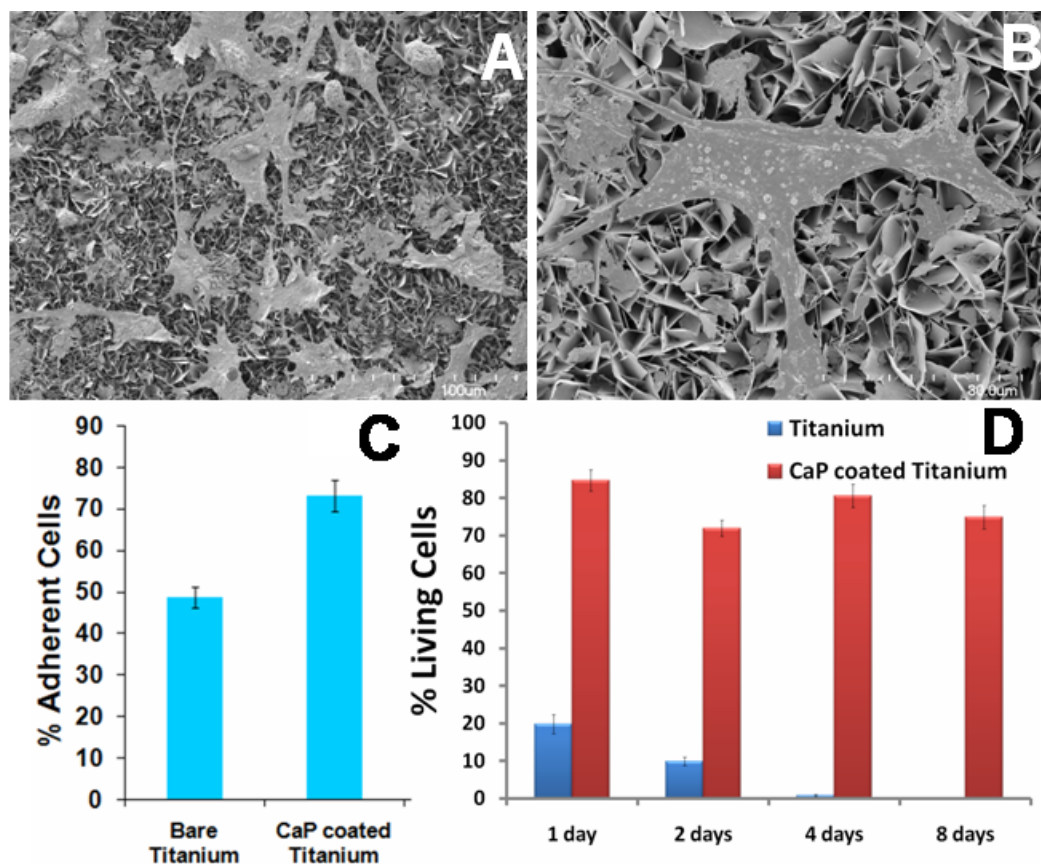


Figure 5.6: A) and B) SEM micrographs of pre-osteoblastic cells adhered onto struvite-calcium phosphate coating after 8 days. C) 2h cell attachment test. D) Live/Dead Viability/cytotoxicity Assay.

5.1.5- Discussion

In the present study we investigated the use of a reactive magnesium metal coating as both a nucleation site and source of reactant cations for the formation of an apatitic layer on a titanium metal surface via a low-temperature aqueous deposition technique. Bioceramic coatings were produced by immersing magnesium sputter-coated titanium substrates in ADP and CaP solutions through chemical reactions between the magnesium metal and the ionic components of the solutions. We demonstrated an approach to produce reactant stable struvite coatings that were able to be subsequently replaced by a layer of calcium phosphate. PBS and SBF solutions were able to form only

patchy coatings, despite the fact that the magnesium coating was able to react with them. These results indicate that the salts resulting from the reaction between magnesium metal and the ions present in SBF and PBS were mechanically and/or chemically unstable on the metal surface.

The Pilling-Bedworth ratio, (P-B ratio) R , of a metal oxide is defined as the ratio of the volume of the metal oxide (V_{oxide}), which is produced by the reaction of metal and oxygen, to the consumed metal volume (V_{metal}):

$$R \equiv \frac{V_{\text{oxide}}}{V_{\text{metal}}} = \frac{Md}{amD}$$

M and D are the molecular weight and density of the metal oxide whose composition is (Metal)_a(oxygen)_b; m and d are the atomic weight and density of the metal. When R values are less than 1, metal oxides tend to be porous and non-protective because they have insufficient volume to cover the whole metal surface, whereas excessively large R values cause large compressive stresses in the metal coat that are likely to lead to buckling and spalling. However, an R value of ~ 1 is indicative of a protective stable oxide [28]. Magnesium quickly develops a protective oxide film upon exposure to air, but magnesium oxide (MgO) with the P-B ratio of 0.81 [28] only provides limited protection to further corrosion. In wet air and aqueous solutions, oxide and hydroxide layers (MgO/Mg(OH)₂) can form spontaneously on the surface. The morphology and structure of the films formed on the pure magnesium after immersion in water is known to have a tri-layered structure with an inner cellular structure layer of 0.4–0.6 μm , a middle dense layer of 20–40 nm (MgO layer) and an outer platelet-like layer (Mg(OH)₂ layer). This film has a P-B ratio of 1.77 and does not provide corrosion protection [29]. Also, pure magnesium and its alloys, magnesium oxide and hydroxide films have poor resistance to pitting corrosion in aqueous solutions containing aggressive anions such as chloride [30]. Probably for this reason, all the coatings produced with solutions containing chloride ions were unsatisfactory (Samples A-F). Indeed, the

minimal corrosion rate of Pure Mg in SBF is about 2mm/yr [31] or 19-44mg/cm²/day [32], for this reason, the 3 µm thick magnesium layer was totally dissolved in SBF solutions in less than 24h. However, in this study, the ADP solution did not completely corrode the sputtered magnesium, by contrast, it formed a stable coat of struvite that seemed to protect the unreacted magnesium beneath. Other studies have reported that certain anions such as phosphate, borate, sulphate and fluoride, are able to produce coatings with an anti corrosive effect on magnesium alloys [33, 34]. This may explain why ADP solutions were able to successfully produce stable coatings. In Figure 5.7 we present a scheme explaining the proposed mechanism behind the coating formation.

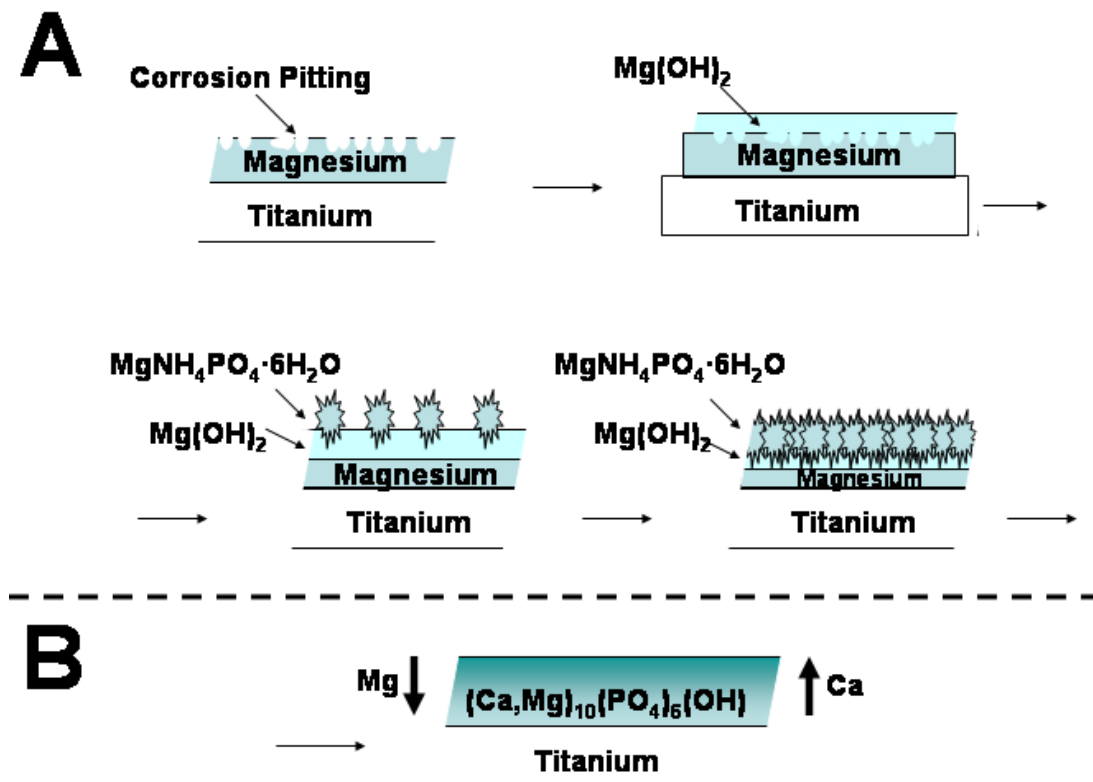
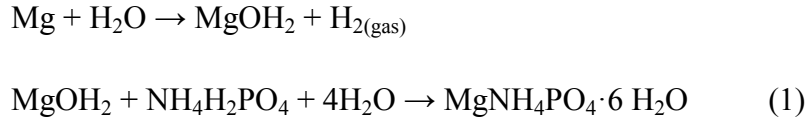


Figure 5.7: Proposed mechanism of: A) struvite coating formation on magnesium sputtered titanium after placement in ADP solution; B) and the subsequent transformation into hydroxyapatite after incubation in CaP solution.

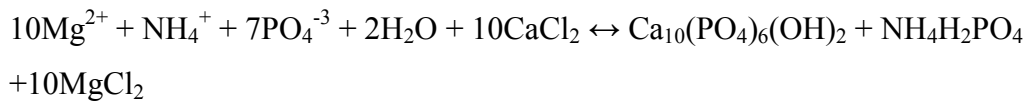
The solubility product constant (K_{sp}) of $MgHPO_4 \cdot 3H_2O$ (1.5×10^{-6}) and magnesium hydroxide (1.5×10^{-11}) are several orders of magnitude higher than that of struvite ($\sim 30.2 \cdot 10^{-14}$), for this reason struvite coatings were initially the most stable at neutral pH and deposited via the following reaction (See Figure 5.7):



Nevertheless upon immersion in physiological fluids, struvite coatings dissolved faster. The equilibrium established in a saturated solution of struvite is:



The solubility product of struvite at $37^\circ C$ ($\sim 30.2 \cdot 10^{-14}$) is much higher than most calcium phosphate bioceramics such as beta tricalcium phosphate 2.07×10^{-33} and hydroxyapatite 10^{-53} [35,36]. Therefore in the presence of calcium ions, struvite is likely dissolve and reprecipitate as a less soluble calcium phosphates phase:



Hence, struvite coatings enhanced the formation of apatite resembling bioactive surfaces. Magnesium ions are known to kinetically hinder the nucleation and subsequent growth of hydroxyapatite ($Ca_{10}(PO_4)_6(OH)_2$; HAP) by competing for lattice sites with the

chemically similar but larger calcium ions. However, this is highly dependent on the concentrations of both calcium and magnesium ions in the system. In this study the CaP precipitation solution had a concentration of calcium ions (2mM) 2 orders of magnitude higher than the theoretical maximum magnesium content in the system [37].

Bare smooth titanium is known to have a limited capacity in enhancing osteoblast adhesion and survival over time [38] which is similar to our findings (Figure 5.6). However, in this study the CaP coating formed on magnesium coated titanium substrates enhanced osteoblast survival and adhesion on the metal surface (Figure 5.6).

Extensive research has been carried out on the precipitation of struvite crystals for industrial use in wastewater treatment plants and in the production of fertilizers [39-41]. Significantly, studies in these fields have revealed that struvite precipitates adhere well to metallic surfaces [42]. The present study demonstrates the first attempt in the literature to effectively precipitate struvite crystals onto metallic surfaces for biomaterial applications and be used as nucleation sites to precipitate calcium phosphate coating.

5.1.6- Conclusion

We have shown that it is possible to form biocompatible surface coatings on metals through a low temperature aqueous deposition technique via the corrosion of a sputter coated reactive metal layer. Resulting surfaces were examined in terms of adhesion strength, cell adhesion and coating microstructure. This process shows good promise in producing enhanced coatings with many advantages over currently used techniques which include the ability to coat complex shapes, alter surface chemistry and the potential to incorporate biologically active compounds.

5.1.7-Acknowledgements

The authors would like to thank Mr. Jeffrey LeDue and Prof. Peter Grütter for their help and advice. The authors also acknowledge financial support from NSERC Strategic grant in collaboration with Terray Corporation, (Arnprior, Ontario, Canada), the "Fundacion Espanola para la Ciencia y Tecnologia" (FT); and the Canada Research Chair program (JB).

5.1.8- References

- [1] Lemons JE. Hydroxyapatite coatings. Clin Orthop 1988;235:220–3.
- [2] Frosch KH, Stürmer KM. Metallic Biomaterials in Skeletal Repair. Eur J Trauma 2006;32:149–59
- [3] Harvey EJ, Bobyn JD, Tanzer M, Stackpool GJ, Krygier JJ, Hacking SA. Effect of flexibility of the femoral stem on bone-remodeling and fixation of the stem in a canine total hip arthroplasty model without cement. J Bone Joint Surg Am 1999;81A(1):93–107.
- [4] Puleo DA, Huh WW. Acute toxicity of metal ions in cultures of osteogenic cells derived from bone marrow stromal cells. J Appl Biomater 1995;6:109–16.
- [5] Jacobs JJ, Hallab NJ, Skipor AK, Urban RM. Metal degradation products: a cause for concern in metal-metal bearings? Clin Orthop Relat Res 2003;417:139–47.
- [6] Wang ML, Nesti LJ, Tuli R, Lazatin J, Danielson KG, Sharkey PF, et al. Titanium particles suppress expression of osteoblastic phenotype in human mesenchymal stem cells. J Orthop Res 2002;20: 1175–84.
- [7] Lhotka C, Szekeres T, Steffan I, Zhuber K, Zweymuller K. Four-year study of cobalt and chromium blood levels in patients managed with two different metal-on-metal total hip replacements. J Orthop Res 2003;21:189–95.
- [8] Wei M, Ruys AJ, Swain MV, Kim SH, Milthorpe BK, Sorrell CC. Interfacial Bond Strength of Electrophoretically Deposited Hydroxyapatite Coatings on Metals. J Mater Sci Mater Med 1999;10: 401–9.
- [9] Park JH, Lee DY, Oh KT, Lee YK, Kim KM, Kim KN. Bioactivity of calcium phosphate coatings prepared by electrodeposition in a modified simulated body fluid. Mat Lett 2006;60: 2573–7.
- [10] Yamashita K, Yonehara E, Ding X, Nagai M, Umegaki T, Matsuda M. Electrophoretic Coating of Multilayered Apatite Composite on Alumina Ceramics. J Biomed Mater Res (Appl Biomater) 1998;43: 46–53.

- [11] Coathup MJ, Bates P, Cool P, Walker PS, Blumenthal N, Cobb JP. Osseomechanical induction of extra-cortical plates with reference to their surface properties and geometric designs. *Biomaterials* 1999;20(8): 793-800.
- [12] Lin FH, Hsu YS, Lin SH, Sun JS. The effect of Ca/P concentration and temperature of simulated body fluid on the growth of hydroxyapatite coating on alkali-treated 316L stainless steel. *Biomaterials* 2002;23(19): 4029-38.
- [13] Kalita VI, Gnedovets AG. Plasma Spraying of Capillary Porous Coatings: Experiments, Modeling, and Biomedical Applications. *Plasma Process Polym* 2005;2: 485-92.
- [14] Habibovic P, Barrère F, Van Blitterswijk CA, de Groot K, Layrolle P. Biomimetic Hydroxyapatite Coating on Metal Implants. *J Am Ceram Soc* 2002;85(3): 517-22.
- [15] Layrolle P, Francois J, de Groot K. Method for coating medical implants. US Patent No. 6733503, 2004.
- [16] Xue WC, Liu X, Zheng XB, Ding C. In vivo evaluation of plasma-sprayed titanium coating after alkali modification. *Biomaterials* 2005;26:3029-37.
- [17] Xue WC, Zheng X, Liu X, Ding CX. Osseointegration of plasma-sprayed titanium coating after alkali modification. *J Inorg Mater* 2005;20:1275-80.
- [18] Glassman SD, Dimar JR, Carreon LY, Campbell MJ, Puno RM, Johnson JR. Initial fusion rates with recombinant human bone morphogenetic protein-2/compression resistant matrix and a hydroxyapatite and tricalcium phosphate/collagen carrier in posterolateral spinal fusion. *Spine* 2005;30(15): 1694-98.
- [19] Uchida M, Oyane A, Kim HM, Kokubo T, Ito A. Biomimetic coating of laminin-apatite composite on titanium metal and its excellent cell-adhesive properties. *Adv Mater* 2004;16(13): 1071-4.
- [20] Stigter M, de Groot K, Layrolle P. Incorporation of tobramycin into biomimetic hydroxyapatite coating on titanium. *Biomaterials* 2002;23(20): 4143-53.

- [21] Narayanan R, Seshadri SK, Kwon TY, Kim KH. Calcium phosphate-based coatings on titanium and its alloys. *J Biomed Mater Res B Appl Biomater*. 2008;85(1):279-99.
- [22] Kramer G, Klingler HC, Steiner GE. Role of bacteria in the development of kidney stones. *Curr Opin Urol* 2000;10(1):35-8.
- [23] Osborne CA, Lulich JP, Polzin DJ, Allen TA, Kruger JM, Bartges JW, et al. Medical dissolution and prevention of canine struvite urolithiasis: twenty years of experience. *Vet Clin N Am—Small Anim Pract* 1999;29:73–111.
- [24] Nadeem U. Rahman, Maxwell V. Meng, and Marshall L. Stoller. Infections and Urinary Stone Disease. *Curr Pharmaceut Des* 2003;9:975-81.
- [25] Zimmermann M. Magnesium ammonium phosphate cement composition. United States Patent No. 7115163, 2006.
- [26] Kokubo T, Takafama H. How useful is SBF in predicting in vivo bone bioactivity? *Biomaterials* 2006;27:2907-15.
- [27] ASTM D 3359 -08. Standard Test Methods for Measuring Adhesion by Tape. In: Annual book of ASTM standards, vol. 03.02. Philadelphia, PA, USA: American Society for Testing and Materials, 1995. p. 48–58.
- [28] Pilling NB, Bedworth RE. The oxidation of metals at high temperature, *J Inst Metals* 1923;29: 529–582.
- [29] Schmutz P, Guillaumin V, Lillard RS, Lillard JA, Frankel GS. Influence of dichromate ions on corrosion processes on pure magnesium . *J Electrochem Soc* 2003;150 (4) :B99
- [30] Fairman L, West JM. Stress corrosion cracking of a magnesium aluminium alloy. *Corros Sci* 1965; 5(10): 711-6.
- [31] Wang Y, Wei M, Gao J, Hu J, Zhang Y. Corrosion process of pure magnesium in simulated body fluid. *Mat Lett* 2008;62(14): 2181-4

[32] Song G, Song S. A Possible Biodegradable Magnesium Implant Material. Adv Eng Mat DOI: 10.1002/adem.200600252

[33] Chen J, Wang J, Han E, Dong J, Ke W. AC impedance spectroscopy study of the corrosion behavior of an AZ91 magnesium alloy in 0.1 M sodium sulfate solution. Electrochimica Acta 2007; 52(9): 3299-309.

[34] Duan H, Yan C, Wang F. Effect of electrolyte additives on performance of plasma electrolytic oxidation films formed on magnesium alloy AZ91D. Electrochim Acta 2007;52: 3785–93.

[35] Aage HK, Andersen BL, Blom A, Jensen I. The solubility of struvite. J Radioanal Nucl Chem 1997;223(1): 213 – 5.

[36] Larsen MJ, Jensen SJ. The hydroxyapatite solubility product of human dental enamel as a function of pH in the range 4.6-7.6 at 20 degrees C. Arch Oral Biol 1989;34(12):957-61.

[37] Salimi MH, Heughebaert JC, Nancollas GH. The Crystal Growth of Calcium Phosphates in the Presence of Magnesium Ions. Langmuir 1985;1:119-22.

[38] Kudelska-Mazur D, Lewandowska-Szumieł M, Komender J. Human osteoblast in contact with various biomaterials in vitro. Ann Transplant. 1999;4(3-4):98-100.

[39] Pastor L, Marti N, Bouzas A, Seco A. Sewage sludge management for phosphorus recovery as struvite in EBPR wastewater treatment plants. Bioresource Technol 2008; 99(11):4817-24.

[40] Fattah KP, Mavinic DS, Koch FA, Jacob C . Determining the feasibility of phosphorus recovery as struvite from filter press centrate in a secondary wastewater treatment plant. Environ Sci and Health - Part A: Toxic/Hazardous Subs and Environ Eng 2008;43(7):756-64.

[41] Bhuiyan MIH, Mavinic DS, Koch FA. Phosphorus recovery from wastewater through struvite formation in fluidized bed reactors: A sustainable approach. *Water Sci Technol* 2008;57(2):175-81.

[42] Le Corre KS, Valsami-Jones E, Hobbs P, Jefferson B, Parsons SA, Struvite crystallisation and recovery using a stainless steel structure as a seed material. *Water Res* 2007; 41(11):2449-2456

CHAPTER 6: Discussion and Conclusion

With the increasing life expectancy and due to younger patients undergoing orthopaedic procedures, the need for better bone repair grows in importance. Magnesium metal possesses mechanical strength close to bone, and its degradable properties make it potentially useful as temporary scaffold to take over the load during bone healing. However, due to their fast degradation rate, attempts on tailoring the mechanical properties of magnesium implants by alloying and physical or chemical alteration of the surface have been reported. However, the rapid corrosion rate and release of hydrogen gas remain a major concern. In order to stabilize and eventually reduce the degradation rate of magnesium, the approach used in this study was to form a magnesium phosphate layer on the surface of magnesium sputtered titanium. This was performed through a low temperature aqueous precipitation process by submerging the sputtered metal in phosphate solutions.

This work highlights the advantage of transforming the outer surface layer of magnesium into magnesium phosphate, which was demonstrated to slow down the degradation of magnesium. This project also demonstrated that what sets the magnesium phosphates apart from the calcium phosphates are their larger degree of hydration at a given Mg/P molar ratio. As shown in Table 3.6, struvite and newberyite are the two most studied soluble phosphates. However, the main difference between these two compounds is that the solubility product constant (K_{sp}) of struvite is significantly lower than that of newberyite, which makes it more stable to form coatings at physiological conditions. Furthermore, struvite acts as nucleation site for calcium phosphate and not with any of the other tested PBS or SBF solutions as the calcium ions tend to participate into an ion substitution mechanism where they replace magnesium to form more stable calcium phosphates. Furthermore, struvite is formed naturally *in vivo* as stone through an interesting mechanism of biological calcification [Khan *et al.* 1988 and McLean *et al.* 1985, Lian *et al.* 1977].

In conclusion, the present study provides insights regarding the potential use of magnesium phosphate coatings in biomedical applications and explores their further use as new biomaterials. The use of reactive alkali metal coatings as nucleation sites and source of coating reactant ions appeared to show great promise as a method for creating inorganic coatings on substrates at room temperature. Although *in vitro* models have the advantage of isolating the effects of osteoblast cells on the magnesium phosphate precipitates and coatings, they are simplified models of the processes happening *in vivo*. Therefore, conclusions should be made with caution and *in vivo* studies should be repeated to confirm these results.

Chapter 7: Future Research

This thesis provided insights on the formation mechanism of magnesium phosphate precipitates as well as their application as bioceramics coatings on metallic implants. However, further work on *in vivo* implant interaction would contribute to the improvement of the current model as well as the exploration of other applications and more complex system of magnesium phosphates. Preliminary results and research directions for the continuation of this project are proposed in this chapter.

7.1 Preliminary *in vivo* results

This section briefly highlights preliminary *in vivo* results of magnesium phosphate coated metal. Optimal coating conditions determined *in vitro* were studied *in vivo*, and compared with lab grade and pure magnesium metals.

As previously mentioned, rapid corrosion of magnesium at physiological conditions and the release of hydrogen gas have been a source of problem for decades. Many alternatives have been tried to counter this problem, such as by alloying and physically altering the surface. However, the rate of degradation is still too high and the production of hydrogen gas hinders bone formation and growth. Nevertheless, its lightweight property, low density (compared to other commonly used metallic implants), role in human metabolism, and the natural presence of magnesium in bone tissue, makes it suitable for bone repair. The next step of this project was to investigate the magnesium phosphate coated low grade magnesium alloy *in vivo* and compare with pure and low grade alloyed magnesium metals.

Materials and Methods

Three of each group of magnesium samples were used for this study; i) 99.98% pure magnesium (10 x 5 x 5 mm blocks, *Magnesium Elektron*, New Jersey, USA) ii) \geq 99.5% magnesium ribbon (0.2 mm thick cut into 30 x 3 mm strips, *Sigma-Aldrich*,

Missouri, USA) and iii) magnesium phosphate coated magnesium ribbon. They were first cleaned by ultrasound for 5 min in 100% ethanol followed by 100% acetone. Then they were dipped in 0.1M H₃PO₄ for 20 sec while rinsing with H₂O in between steps and left to air dry. The coated magnesium samples were prepared by immersing in a 3:1 molar ratio of 1M PO₄⁻: 1M NH₄⁺ solution for 24h at physiological conditions.

The sectioned pieces were then polished with a silica nitride paper and rinsed with distilled water.

Characterization

Characterization of the surfaces was performed using the VP-SEM, EDX and X-Ray. X-Rays were taken from the top and both sides of the rats after one week implantation.

Wistar Rats

Wistar rats (weight=350g) were selected and allowed to acclimatize for 1 week prior to surgery. The cages containing each animal were maintained in a controlled temperature (23 ± 1 °C) room with light/dark cycles of 12 h. The rats were anaesthetized with standard anesthetic cocktail consisting of ketamine hydrochloride (60 mg/kg) and xylazine (5 mg/kg), administered intraperitoneally. Surgery was performed using aseptic techniques. The animals were anaesthetized with urethane 37.5% (0.4 mL/100 g) and the samples of the soft tissues were removed by surgical technique. After this, these samples were immersed in 4% paraformaldehyde/0.1 M phosphate-buffer solution for 24 h, and processed for histological analysis. In sequence, they were imbedded in paraffin, cut into 6 µm thick sections and stained with hematoxylin and eosin. The histological sections were analyzed by microscope (Leica DMRB, Germany) connected to a digital camera (Olympus DP11, USA).

Subcutaneous Implantation

Subcutaneous implantation in rats for 4 weeks were performed at University of Sao Paulo, Brazil. Four rats were used as implant models. One of each uncoated and

coated magnesium ribbon samples were inserted in three rats. The fourth rat had all three pure magnesium implanted.

Preliminary Results

Percent Weight Loss After Implantation

Preliminary data are presented in Figure 7.1. Magnesium ribbon showed variable results, as Ribbon 1 had a ~2mm hole perforating its thickness, whereas the other had a gain in weight. However even a weight gain is indicative of corrosion as hydroxides or phosphates are formed. Differences may have been due to differences in implant location. No gas pockets were observed. Coated magnesium appeared to have a slower degradation rate and be more consistent. However, since only duplicates were performed, further work is required to explore these interesting and unexpected findings.

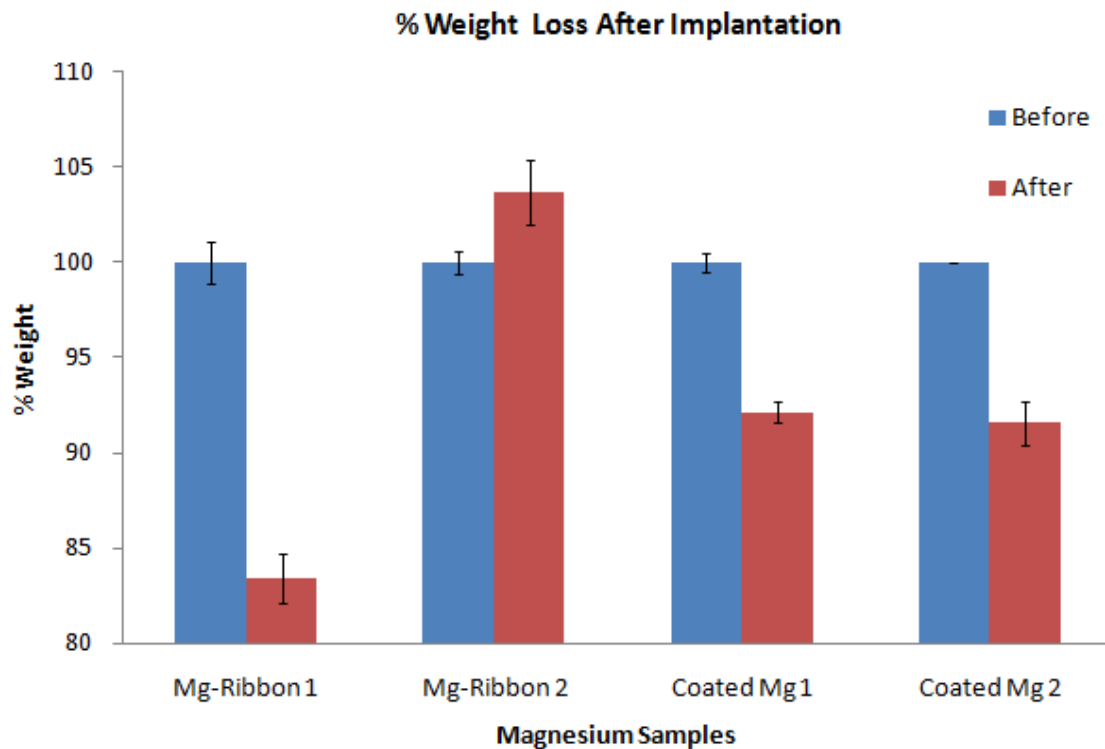


Figure 7.1: Comparison of mean percent weight loss (\pm sd) after four weeks implantation of low grade magnesium and coated magnesium. Note: Pure magnesium is not included due to insufficient sample numbers.

X-Ray Images

Magnesium ribbons were undetectable on X-Rays irrespective of animal orientation making monitoring or degradation without animal sacrifice impossible (Figure 7.2)

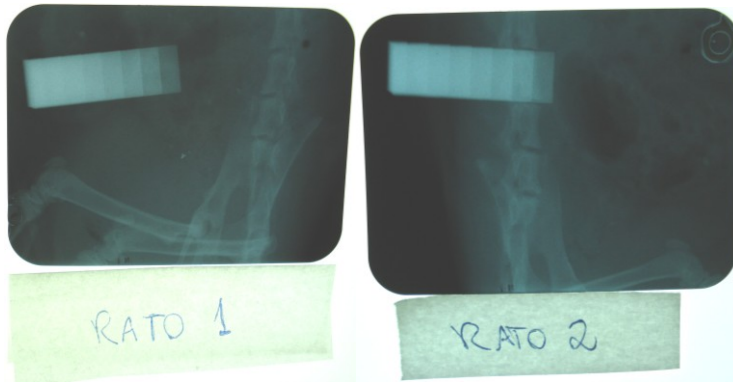


Figure 7.2: X-ray images of implants *in vivo*. However, due to the low radiopacity of magnesium, the samples could not be observed under X-Ray images.

SEM micrographs and EDX analysis

After implantation for 4 weeks, lab grade magnesium ribbon showed evidence of formation of a sodium –magnesium-hydroxide phosphate compound. The coated ribbon however differed in that a calcium phosphate had clearly formed. Little change in surface morphology occurred in this sample. However, the uncoated magnesium had a thick and cracked coating (Figure 7.3).

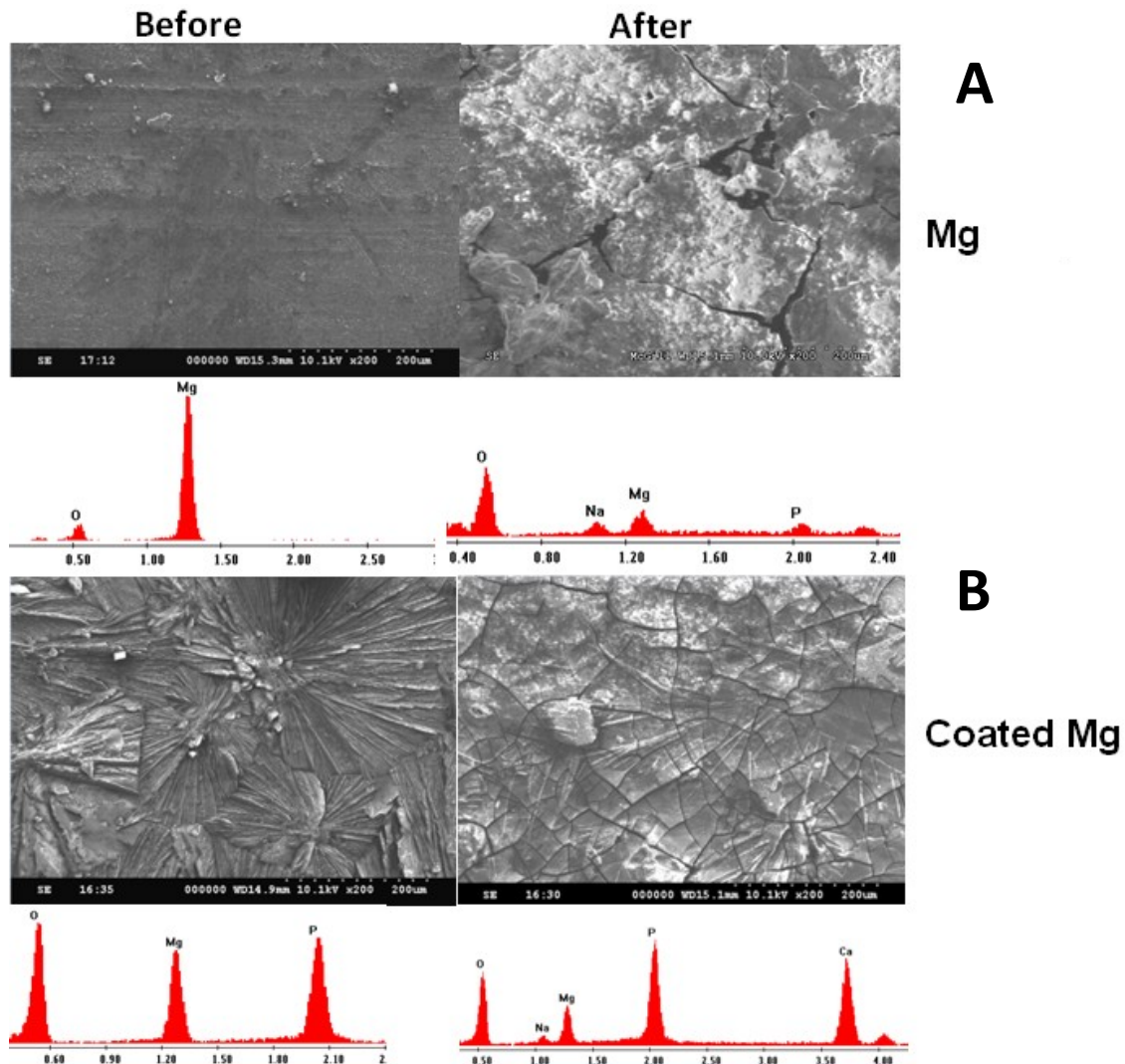


Figure 7.3: SEM micrographs and EDX analysis of A) low grade magnesium alloy and B) coated magnesium before and after four weeks implantation.

Discussion and Conclusion

Figure 7.1 indicated that coating the metal with magnesium phosphate shows less degradation of the surface *in vivo*. Furthermore, SEM micrograph and EDX analysis reveals the formation of apatite on the surface of coated magnesium which we speculate that they are biocompatible. It was also observed under histology that there was no apparent inflammation of the surrounding tissue around the implant, which makes them non-toxic. However, due to the very low radiopacity of magnesium, it was not visible under X-ray. It is highly suggested that these tests would need to be reproduced with more samples and rats in order to get more accurate results and draw better conclusion.

7.2 Magnesium Phosphate Cements

Other promising directions of this project were the potential application of magnesium phosphate as biodegradable cement materials. Different molarity of hydrogen phosphate was reacted with magnesium oxide powder to form a paste. It was found that 5M of phosphoric acid with MgO formed a very strong cement of approximately 16 MPa. These magnesium phosphate cements also did not degrade in water, but rather continued the reaction to form stronger cement. However, the reaction occurs too rapidly and releases gas, which produces inconsistent and heterogeneous paste. Other acids are currently being assessed to reduce the reaction rate to have more controllable and reproducible paste cement. Recently, Argonne National Laboratory developed a magnesium potassium phosphates (Ceramcrete), to fulfill the need for materials to stabilize and encapsulate radioactive and hazardous waste streams. A magnesium phosphate is under development for veterinary applications but little data has been published. Furthermore, effects of a magnesium adhesive cement on bone stability and healing following a metatarsal osteotomy in horses have also been investigated. [Waselau *et al.* 2007]